

PREDICTIVE CONTROL OF HEAT PUMP AND THERMAL ENERGY STORAGE FOR FLEXIBLE HEATING

A Thesis

Presented to the Faculty of the Graduate School
of Cornell University

in Partial Fulfillment of the Requirements for the Degree of
M.S.

by

Kartikay Gupta

August 2018

© 2018 Kartikay Gupta
ALL RIGHTS RESERVED

ABSTRACT

Mass electrification of the residential and commercial heating sector using heat pumps and thermal energy storage is a crucial step towards the development and operation of smart grids. An aggregation of heat pumps can provide an alternate source of frequency regulation by generating flexibility on the demand side as opposed to inefficient natural gas generators that are a source of supply side flexibility. This in turn can facilitate greater incorporation of power generated from clean but intermittent sources of energy such as wind and solar. To this end, a hierarchical control scheme is introduced that will enable an aggregator to tap into the inherent flexibility associated with a portfolio of variable speed heat pump/thermal storage subsystems. This work concentrates on the development of a model based predictive controller operating on the subsystem level and its integration into the global control architecture. Additionally, the value of formulating the performance cost optimization function and the system dynamics equation as a mixed integer program is explored. The aforementioned formulation facilitates the use of simplified, yet comprehensive, dynamic heat pump performance models and at the same time addresses the problem of heat pump operation in the compressor dead-band range. The simulations also highlight the power-tracking functionality of the developed controller when it is integrated with higher level controllers in the hierarchical control scheme.

Index Terms - Variable Speed Heat Pump, Thermal Energy Storage, Frequency Regulation, Economic Model Predictive Control, Mixed Integer Programming

BIOGRAPHICAL SKETCH

Kartikay Gupta is a native of Lucknow, a city situated in the state of Uttar Pradesh, India. He completed his high school in the same city and then decided to pursue a Bachelor's Degree in Mechanical Engineering from VIT University in Tamil Nadu, India in the year 2012. During his time at VIT, Kartikay was extensively involved in the development of formula type electric cars for Formula Student competitions and also led a team of undergraduate engineering students to the Formula Student competition in Germany. During his senior year, he interned at Research Designs and Standards Organization which is the research and development wing of Indian Railways. His project pertained to conducting life cycle analysis of different fuel/locomotive systems. He graduated from VIT in May 2016 and then entered the Master of Science program at Cornell in August 2016. Since then he has been working as a graduate researcher at the Energy & Environment Research Lab and his primary interests lie in the area of intelligent energy systems and machine learning.

ACKNOWLEDGEMENTS

I would like to initiate this acknowledgement by thanking my advisor, Prof. K. Max Zhang for his constant guidance and for giving me the opportunity to work on this interesting project. His patience and support throughout the course of this study is much appreciated. I take this opportunity to also express my deep gratitude to Mr. Kevin Kircher, a MAE PhD student working with Prof. Zhang. His valuable inputs and suggestions have been instrumental in ensuring the steady progress of this research. My gratitude is also extended to Prof. Jefferson Tester who very kindly agreed to be a member of my committee and also gave me an opportunity to present my work at the Earth Energy seminar in Fall of 2017. His suggestions during the preliminary stages of the project helped me structure my work. I would also like to thank all the members of the Energy & Environment Research Lab for their constructive suggestions with regard to my research. Special thanks to Liyan Cao for his help with the controlled plant configuration diagram. Also thanks to all my friends here at Cornell for ensuring that things did not get too monotonous. Finally, I would like to express my appreciation to my parents. Their constant encouragement and faith in me is simply amazing. This study, and so many other things, would certainly not have been possible without their support.

TABLE OF CONTENTS

Biographical Sketch	iii
Acknowledgements	iv
Table of Contents	v
List of Figures	vi
List of Tables	ix
List of Abbreviations	x
1 Introduction	1
1.1 Electrification of the Heating Sector	1
1.2 Utility of Thermal Energy Storage in Electrified Heating	3
1.3 Utility of Electrified Heating in Smart Grids	5
2 Contribution and Organization of this Work	7
2.1 Hierarchical Control Strategy for Aggregation	7
2.2 Model Based Predictive Control at Subsystem Level	9
3 Methodology	14
3.1 Dynamics of the Heat Pump - Thermal Storage System	14
3.1.1 System Configuration	14
3.1.2 Thermal Energy Storage Model	16
3.1.3 Heat Pump Power Input and Thermal Output	20
3.1.4 Space Heating Demand	25
3.2 Development of Model Predictive Controller	26
3.2.1 State Space Representation of the System	26
3.2.2 Performance Cost Modeling	28
3.2.3 Open-Loop Optimal Control Problem	30
4 Simulation Results & Discussion	32
4.1 Value of Mixed Integer Approach	37
4.2 Power Tracking Performance of MPC Controller	43
5 Conclusion	46
A Elements of Model Predictive Control	49
References	52

LIST OF FIGURES

1.1	Residential Energy Use Breakdown, 2009. The pie charts show that the energy consumption for space heating is the highest in comparison to other sources.	1
1.2	Percentage Breakdown of Space Heating Fuel Used, 2009. From the stacked bar plots, it is evident that most of the residential space heating comes from burning of fossil fuels such as natural gas and fuel oil.	2
1.3	Basic Heat Pump Operating Cycle	3
2.1	Information Flow in the Proposed Control Architecture. This hierarchical control scheme will enable a portfolio of heat pump/thermal storage subsystems to participate in grid frequency regulation market. This work pertains to the development of the slow local controller.	8
3.1	Controlled Plant Configuration. This represents the system being controlled which consists of a VSHP connected to a thermal storage in series configuration. The heating demand of the space is directly met by the thermal storage.	14
3.2	Schematic of the Stratified Thermal Storage System.	16
3.3	VSHP Performance Curves. Plot (a) shows that the heat pump COP increases with the increase in ambient temperature. Plot (b) shows the inverse relationship between COP and condenser temperature. Plots (c) and (d) show the variation of compressor power and heat pump thermal output with ambient temperature. The cumulative effect of these correspond to an increase in COP with increase in ambient temperature. These are in tandem with the operation of a heat pump in real world.	24
3.4	Rendered CAD Model of the Residential Low Rise Apartment. This prototype is simulated in EnergyPlus for obtaining the heating profile that is used in equation 3.18	26
4.1	Diurnal Trend of Non-Stationary Temperature Data. The similar shapes of temperature profiles for 5 days suggest the presence of daily seasonality which makes the data non-stationary. This suggests that ARIMA models coupled with data differencing techniques or in other words SARIMA models need to be used for making diurnal temperature predictions.	34
4.2	Hyper parameter Tuning for Random Forest. This shows the results of 5-fold cross validation used for determining the optimal number of decision trees	35

4.3	Predictive Performance of SARIMA and Random Forest Models. These plots give an estimate of the performance of algorithms used for making diurnal temperature and heating load predictions for 100 Monte Carlo Simulations. The dotted vertical lines in the plots denote the mean of the plotted values.	36
4.4	True and Predicted Values of the Exogenous Disturbances. The top plot shows the predicted and true values of the ambient temperature for the simulation day. The bottom plot does the same for heating load. The predicted values are used for making state predictions in the MPC horizon while the true values are used for updating the system state at each MPC iteration. With a mean square error of 0.67 for temperature predictions and 0.165 for heating load predictions, the quality of predictions is good. This fact is crucial as good predictions ensure that the control policy obtained is optimal. Bad predictions can lead to sub-optimal control policies with high system operating costs.	38
4.5	System States and Controls Under the MPC and Prescient Policy. The first plot shows NYSEG’s three tiered i.e. off-peak, on-peak and mid-peak electricity service rate. For plots 2 and 3, the baseline (shown in orange) is computed by solving a certainty equivalence problem and provides a lower bound on the performance of the MPC algorithm. Furthermore, it is observed that the thermal storage is charged during the time of low electricity prices and is ultimately used during the time of high energy prices to meet the heating needs.	39
4.6	System States and Controls Under Mixed Integer and Simple Linear Formulation. The shaded area in the second plot denotes operation in the compressor dead-band as suggested by using the original heat pump performance equations. This issue is adequately addressed by the introduction of binary variables which enable the model avoid operation in the compressor dead band.	40
4.7	Comparison of Heat Pump Power Consumption and Thermal Output Under Mixed Integer and Simple Linear Formulation. The shaded areas in the plots highlight the anomaly associated with using the original heat pump performance models as non-zero power consumption and heat output values are obtained at zero compressor shaft speeds. On the other hand, the mixed integer formulation rectifies this anomaly and drives the pump power consumption and heat output to zero at zero compressor speeds.	41

4.8	Simulation Run Times for Mixed Integer and Simple Linear Formulation. The average run time for mixed integer formulation (14.4 seconds) is slightly greater than that of the linear formulation (12.1 seconds). Thus, the mixed integer formulation can easily be implemented without incurring a significant increase in processing time.	42
4.9	Frequency of Compressor Dead Band Violations under Linear Formulation. The above plot shows the number of control points, as computed by solving the linear formulation, that lie in the compressor dead band range for each Monte Carlo iteration. [1] and [2] tackle this problem by implementing a post-processing step as discussed earlier. Having a mixed integer formulation essentially eliminates this post-processing step.	43
4.10	Tracking Performance of MPC Controller. This plot shows the pump power profiles for different values of the penalty parameter ρ . It is observed that as the value of the tunable parameter increases, the subsystem level controller forces the pump power sequence to inch closer to the reference power trajectory. This behavior proves the effectiveness of MPC framework to closely track the reference power signal from higher level controllers, thereby ensuring that the subsystem can participate in the frequency regulation market.	45
A.1	Receding Horizon Implementation	51
A.2	Model Predictive Control Algorithm	51

LIST OF TABLES

3.1	Fundamental Model Parameters and Exogenous Input Signals .	17
3.2	Coefficients of Fit for Pump Power Consumption and Thermal Output	22
3.3	Regression R-Squared Values	23
4.1	Time Invariant Simulation Parameter Values	32

LIST OF ABBREVIATIONS

RECS	Residential Energy Consumption Survey
ASHP	Air Source Heat Pump
TES	Thermal Energy Storage
EERL	Energy and Environment Laboratory
MPC	Model Predictive Control
EMPC	Economic Model Predictive Control
TOU	Time of Use
VSHP	Variable Speed Heat Pump
COP	Coefficient of Performance
BPS	Building Performance Simulation
IECC	International Energy Conservation Code
SARIMA	Seasonal Auto Regressive Integrated Moving Average
NYSEG	New York State Electric and Gas Corporation

CHAPTER 1

INTRODUCTION

1.1 Electrification of the Heating Sector

According to Energy Information Administration's 2009 Residential Energy Consumption Survey (RECS)[3], the energy used for space heating constituted the major portion of total energy used by households in United States (US). This consumption was much higher for the households situated in Middle Atlantic (MidAtl) area which includes the states of New York state, New Jersey and Pennsylvania as shown in Figure 1.1 below

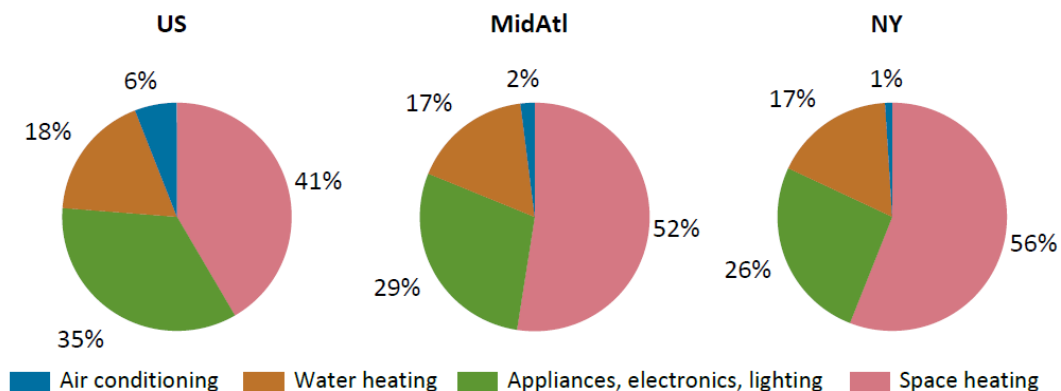


Figure 1.1: Residential Energy Use Breakdown, 2009. The pie charts show that the energy consumption for space heating is the highest in comparison to other sources.

The same survey also reports that most of this space heating came from fossil fuels such as natural gas and fuel oil. The use of electricity as a heating fuel constituted a relatively small portion of the entire mix in case of the MidAtl

region and the contribution was even smaller for New York state as is evident in Figure 1.2.

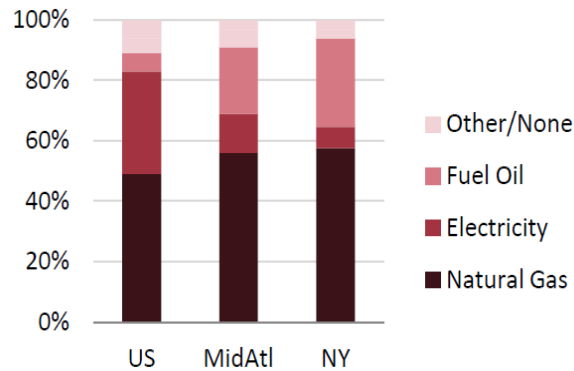


Figure 1.2: Percentage Breakdown of Space Heating Fuel Used, 2009. From the stacked bar plots, it is evident that most of the residential space heating comes from burning of fossil fuels such as natural gas and fuel oil.

Fossil fuel powered heating systems are preferred by consumers because they are comfortable, convenient and reliable. However, they are also responsible for increasing the atmospheric concentration of greenhouse gases which has consequently resulted in global warming. This unwanted climate change has been accompanied by an increased risk of droughts and increased intensity of storms in different parts of the world. In addition to the problem of greenhouse gas emission, there are some safety concerns associated with their use as well as a leak in the case of natural gas systems can potentially lead to an explosion and fire. Fossil fuel powered systems have also been known to adversely affect the air quality at home [4].

The problems associated with natural gas heating systems can be overcome by replacing such systems with heat pumps. Heat pumps are electrically-powered refrigeration devices that are capable of providing both heating and

cooling to a residence. They do not produce heat energy by burning fuel but rather transfer heat from one space to another by working against the temperature gradient. Therefore, during the winters, heat pumps consume electricity and move heat from the cool outdoors into the warm house. Now depending on the source from where they draw heat, heat pumps can be of three types: air-to-air, water source and geothermal. However, the principle of operation is same for all the three types and the basic components of any such system are a compressor, evaporator, condenser, and an expansion valve. Figure 1.3 shows these components are linked together to form the basic heat pump cycle [5].

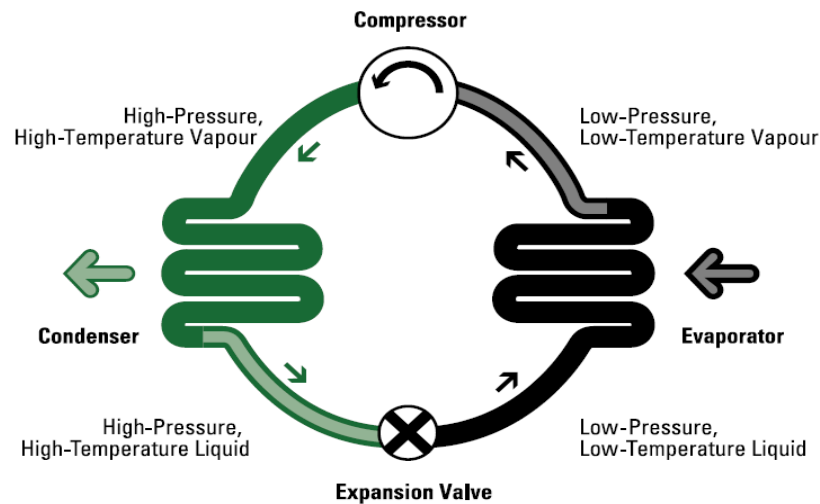


Figure 1.3: Basic Heat Pump Operating Cycle

1.2 Utility of Thermal Energy Storage in Electrified Heating

Despite having advantages such as significantly lower electricity consumption and cleaner operation in comparison to natural gas furnaces, there are some glaring disadvantages associated with the use of a heat pump. For instance,

air-source heat pump (ASHP), which is the most common type of heat pump, cannot be used on subzero days and generally requires some form of supplemental heating. For air to air heat pumps, the backup heat is generally in the form of electrical resistance heaters which are built in the ductwork [6]. The operation of such systems can result in increased peak power demand during extremely cold days, thereby placing enormous stress on the power grid. This phenomenon is thoroughly explored by Liu et. al. [7] and the authors show that electric direct heating, which usually serves as the backup heating for heat pumps, causes high peak electricity loads in all 4 Nordic countries. It is also shown that with lower penetration of electric supplemental heating, the peak demand drops significantly. Fawcett et. al. [8] conduct a similar study where they investigate how heat pump adoption in the residential sector would affect the total and peak electricity demand globally and for individual countries. The authors develop a geographical model that uses historical population-weighted temperature data and assumptions about energy use patterns and efficiency of heat pumps to come up with peak instantaneous demand, calculated at three-hourly time steps. The results show that wide spread penetration of heat pumps will result in very high peak:load ratio in UK, the EU-28 and globally.

To effectively counter the problem of this increased power peak, a thermal energy storage (TES) can be used in tandem with a heat pump instead of electrical resistance heating. The utility of such systems is discussed by Cooper et. al. [9] where the authors show that extensive use of thermal storage devices can reduce the increase in net-peak demand associated with greater adoption of heat pumps in UK dwellings. Moreover, under a dynamic electricity pricing, such a system can also lead to potential cost savings for the system owner as the heating needs of a space can be met by the thermal storage at the time of high

electricity prices instead of the heat pump which can be turned off at that time. This aspect is researched by Renaldi et. al. [10] and their results show that operational cost of a heat pump system without TES are significantly higher than that of an integrated system.

1.3 Utility of Electrified Heating in Smart Grids

The electric power grid transfers power from generators to end consumers using alternating current which oscillates at a frequency of 60Hz [11]. A gap between the power supply and demand causes the grid frequency to change and this can lead to system wide blackouts/brownouts and can cause considerable damage to the power grid. With the increasing penetration of highly intermittent renewable resources of energy such as wind and solar in the power system, the fluctuations in grid and the chances of a mismatch increase significantly. The grid operators manage such fluctuations by sending signals to natural gas generators that ramp up or down to balance the mismatch. This activity of maintaining the oscillating frequency of alternating current within tight tolerance limits is referred to as Frequency Regulation. These regulation resources have inertia associated with them which prevents them from ramping up and down within short time intervals. Thus, the generators are generally maintained on standby which is inefficient and costly.

Mass electrification of the residential heating sector can provide an alternate source of frequency regulation by generating flexibility on the demand side as opposed to natural gas generators that are a source of supply side flexibility. An aggregation of electric heat pumps has great potential as a frequency regulation

asset and numerous studies have been conducted to explore the utility of such systems in enabling greater integration of renewable sources of energy in the energy mix. For instance, Waite et. al. [12] evaluated the effects of coupling large-scale wind power installations in New York state with increased use of electric heat pumps to meet a portion of space heating demand in New York city. Their analysis showed significant increases in wind-generated electricity utilization with increased use of heat pumps, thereby allowing for higher installed capacity of wind power. Georges et. al. [13] from University of Liege, Belgium, also assess the amount of flexibility that can be reserved from a set of residential heat pumps. It is shown that a load aggregator controlling a portfolio of 40000 heat pumps in different Belgian houses can provide up to 100 MW of upward reserve to the power system operator during the winter season. A similar research was conducted by Muhssin et. al. [14] at Cardiff University. The authors developed a dynamic frequency controller that enabled a 5000 heat pump portfolio to vary its cumulative power consumption in response to system frequency. The authors went a step further and integrated the developed controller with a reduced order model of the Great Britain transmission/generation power system to validate the performance of the controllers. The simulation results showed that dynamically controlled heat pumps operating in different bands of Great Britain had significant impact on the system frequency and considerably reduced the dependency on expensive natural gas generators. Comparable studies have been conducted by researchers in countries such as Denmark [15] and Germany [16] and they all have affirmed the importance of heat pumps in facilitating greater inclusion of renewable energy sources in the power grid.

CHAPTER 2

CONTRIBUTION AND ORGANIZATION OF THIS WORK

2.1 Hierarchical Control Strategy for Aggregation

The Energy & Environment Lab (EERL) at Cornell University is actively involved in analyzing the potential of electric heat pumps as a frequency regulation asset. Mr. Kevin Kircher, a PhD student in the mechanical engineering department and a part of EERL, has developed a hierarchical control scheme (Figure 2.1) that can enable an aggregator to control a portfolio of heat pump/thermal storage subsystems to meet the heating needs of its customers and at the same time offer frequency regulation services to the system operator.

The distributed control architecture shown in Figure 2.1 has global and local controllers operating at fast (order of 1 second) and slow (order of one hour) time scales. Local controllers operate on individual heat pump/thermal storage subsystems while the global controllers regulate the collective behavior of the entire portfolio. The control scheme ensures that the portfolio is capable of operating in a two-settlement electricity market [17]. The aggregator will forecast the energy demand for each hour of the following day and submit a bid to the grid operator along with a regulation capacity and regulation price offer. The grid operator will take in similar bids and offers from other market participants and solve a security constrained economic dispatch problem to compute the day-ahead energy prices, regulation capacity commitments, and regulation capacity prices. The aggregator will receive these signals from the system operator and will accordingly schedule the operation of each heat pump/thermal storage subsystem such that the space heating needs of the respective occupants

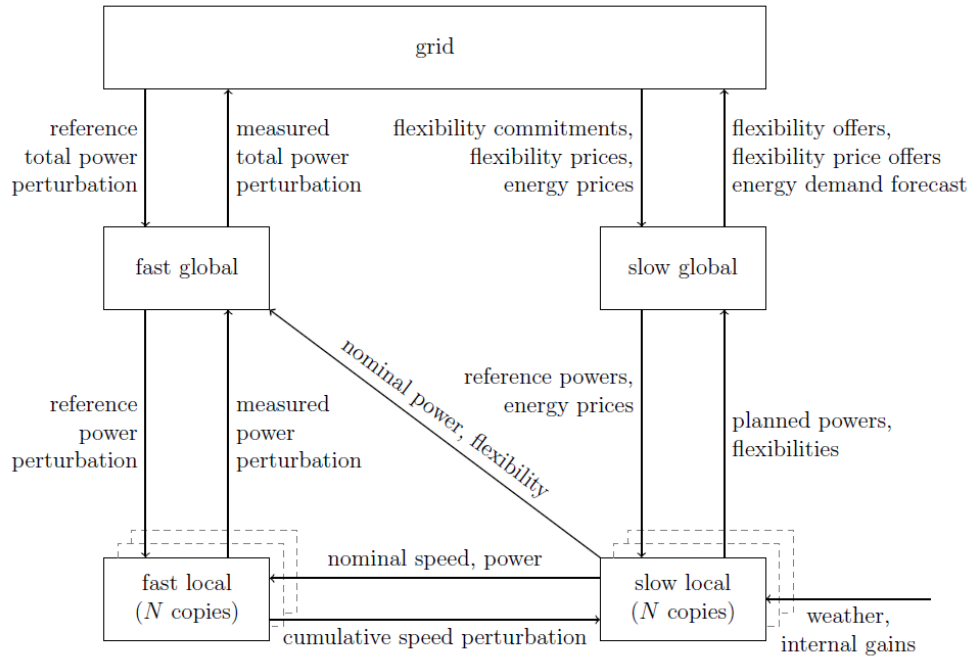


Figure 2.1: Information Flow in the Proposed Control Architecture. This hierarchical control scheme will enable a portfolio of heat pump/thermal storage subsystems to participate in grid frequency regulation market. This work pertains to the development of the slow local controller.

are met at least cost and at the same time the regulation capacity commitments to the grid operator are honored.

The aim of this work is to develop the slow local controller and integrate it into the proposed hierarchical control network. The controller, operating at a subsystem level, will regulate the functioning of a single heat pump/thermal storage system and should be formulated such that it is capable of assisting the slow global controller in meeting the aggregator's two objectives mentioned earlier. This functionality will be achieved in two stages. Initially, the slow local controller will compute a power trajectory in stand alone mode with the objective of meeting the occupant's heating load at a minimal cost. The computed

power trajectory will then be passed to the slow global controller which will receive similar power trajectories from different slow local controllers. The higher level controller will then solve a distributed convex optimization problem with the objective of minimizing the total operating cost and maximizing the revenue from frequency regulation capacity. This will result in an updated power trajectory for each subsystem and this will be communicated back to the slow local controller which will be expected to compute an updated power sequence such that both the energy costs and deviations from the reference power trajectory are minimized.

2.2 Model Based Predictive Control at Subsystem Level

From the previous section, it is evident that the power sequence computed by the subsystem level slow controller plays a crucial role in the entire control scheme. Hence, it is imperative that an optimal sequence is obtained after considering all the objectives. Heuristic and rule based control strategies such as constant proportion control, storage priority control are generally outperformed by optimization based control strategies which are successfully able to navigate the trade-offs between competing objectives. Model Predictive Control (MPC) is one such optimal control strategy based on numerical optimization and since its inception in 1970 by Shell for process control, MPC has come a long way and is one of the most common strategies used for building control. It is capable of controlling large systems with many control variables and provides a systematic method to deal with multiple constraints on inputs and states [18].

Model predictive control of heat pumps coupled with thermal storage de-

VICES has been an area of active research and numerous studies have proven its effectiveness over rule based control in a smart grid scenario. For instance, Awadelrahman et. al. [19] developed an Economic Model Predictive Controller (EMPC) to optimize the heating energy costs in a residential building under the influence of varying electricity price signals. The authors investigated a heating system consisting of an air source heat pump incorporated with a hot water tank as active TES. Their results showed that proposed EMPC achieved greater economic savings by enabling load shifting in comparison to a traditional PID controller. Similar findings were reported by Candanedo et. al. [20] in their work pertaining to the development of a model predictive control strategy for a solar-assisted cold climate heat pump system. The system consisted of two ASHPs with one extracting heat from the ambient air and the other from air preheated by a building-integrated photovoltaic-thermal system. The system was analyzed under a time-of-use (TOU) electricity pricing and MPC algorithm yielded a savings of about 8% in comparison to a rule based control strategy. The economic benefits of MPC have also been confirmed in [21], [22], [23], [24],[25]. Thus, from the literature review, the feasibility of using MPC for heat pump/thermal storage subsystem can be confidently ascertained.

A crucial aspect of this work is the use of simplified, yet comprehensive, formulations for heat pump electric power consumption and heat output. Verhelst et. al. [1] have shown that the use of constant COP models which neglect the dependency of heat pump performance on compressor frequency/RPM, supply water temperature and ambient air temperature, significantly degrade the performance of the predictive controller. The apprehension against the use of constant COP models is reiterated by Bloess et. al. [26] who in their work provide a detailed review of different heat pump modeling approaches for use in

simulating power-to-heat systems that facilitate use of energy from stochastic renewable energy resources. Thus, in this work we use formulations by Kim et. al. [27] for both heat pump power consumption and heat output (Equation 2.1) that are linearly dependent on the compressor shaft rotational speed, ambient temperature and the condenser temperature. These models capture the true dynamics of an ASHP to a considerable extent and at the same time ensure that the computation times are reasonable.

$$\text{HP Power Consumption : } P_t = P(t) = \alpha_1 + \alpha_2 \cdot \omega(t) + \alpha_3 \cdot T_h + \alpha_4 \cdot T_a(t)$$

$$\text{HP Heat Output : } H_t = H(t) = \alpha_5 + \alpha_6 \cdot \omega(t) + \alpha_7 \cdot T_h + \alpha_8 \cdot T_a(t) \quad (2.1)$$

Additionally, this formulation enables us to explore the role of variable speed heat pumps in smart grids which is one of the recommendations given by Fischer et. al. [16] for future research. Despite being comprehensive, the above formulations suffer from a critical drawback as they seem to suggest that the heat pump will consume power/produce heat even when the compressor is not in operation and necessitate that the heat pump be operated in a certain range of speed with no provision of being turned off. In a nutshell, these formulations fail to capture the performance of a heat pump in a real world scenario. Using such a formulation in MPC optimization problem will also result in an erroneous control strategy. Thus, one of the aims of this work is to increase the general applicability and versatility of such simple, yet comprehensive, formulations and this is achieved by introducing binary variables in the MPC optimization problem, thereby transforming it in to a mixed integer problem.

Adopting a mixed-integer programming approach also enables us to effectively address the concept of dead-band in the operation of a modulating heat

pump. The dead band corresponds to heat pump compressor speed range in which the mechanical losses are very high and generally corresponds to 15% of maximum capacity. During operation at very low speeds, the reliability of the bearing used in compressors can be adversely affected due to the decrease in the lubricant film thickness. This can lead to suboptimal system operation and can significantly reduce the life time of the system. This aspect is commonly ignored in most studies where the operating limits are set between 0 and an upper limit which is usually defined by the heat pump manufacturer. A possible work-around this would be to raise the lower bound of operation of the heat pump. However, this would lead to an increase in the operating costs and heat losses. Some studies suggest a clever post-processing step after the optimization results to tackle this issue. If the control input obtained from optimization corresponds to operation in the dead-band range, the heat pump is forced to operate at the manufacturer defined lower limit for a shorter time duration so that an equivalent amount of thermal energy is delivered [1],[2]. Mixed-integer programming provides an alternate way of addressing this problem and essentially eliminates the need of having a post-processing step as the control inputs computed from solving the mixed integer optimization problem either correspond to heat pump being switched off or operation within the prescribed speed limits.

As stated earlier, the slow local controller receives an updated power trajectory from the slow global controller and is expected to recompute a future power sequence such that deviations from this trajectory are minimized. This implies that the MPC framework, controlling a heat pump/thermal storage subsystem, needs to be extended to implement this power tracking functionality. Vrettos et. al. [28] developed such a framework where MPC was used to define local heat pump operating set-points such that energy costs were minimized

while ensuring that a sufficient window existed for participation in grid frequency regulation. The extended MPC framework presented in this work also incorporates a stratified thermal storage in addition to a heat pump, thereby making it an original contribution to the existing literature. The power tracking capability of reformulated MPC problem is shown using a hypothetical reference power trajectory from the slow global controller and the subsystem level controller's behavior in a hierarchical control scheme is quantified.

The organization of this work is as follows. In §3, the physics and economic models that form the core of the MPC strategy are developed. §4 discusses the simulation parameters and results. The machine learning algorithms used for making predictions of exogenous disturbances are also presented in this section. We end by presenting our conclusions in §5 along with recommendations for future work.

CHAPTER 3
METHODOLOGY

3.1 Dynamics of the Heat Pump - Thermal Storage System

3.1.1 System Configuration

An important element of the MPC strategy is to develop a dynamic model that can be used for predicting the future states of the controlled plant. In this case, the system to be controlled comprises of a variable speed heat pump (VSHP) and a thermal energy storage connected in series as shown in Figure 3.1 below:

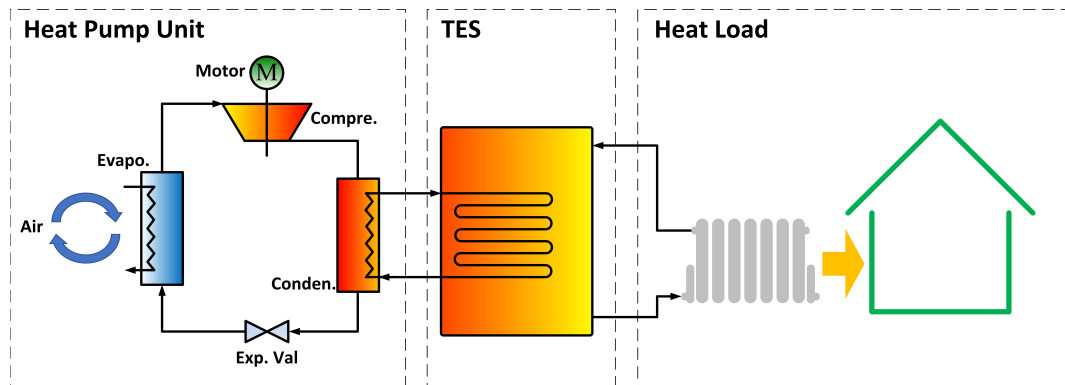


Figure 3.1: Controlled Plant Configuration. This represents the system being controlled which consists of a VSHP connected to a thermal storage in series configuration. The heating demand of the space is directly met by the thermal storage.

The heat pump is used to charge the thermal energy storage which in turn is used to meet the heating demand of a living unit in the building. Depending on the medium that is used to store and release energy, thermal energy storage devices can be broadly categorized as sensible, phase change and stratified. Sensible thermal energy storage devices generally store energy by chang-

ing the temperature of the medium such as ceramics, oil, rock beds etc. Phase change devices store thermal energy as latent heat and provide a greater density of energy storage with a smaller temperature difference between storing and releasing heat than the sensible heat storage method. Stratified thermal energy storage devices generally use water as a heat storage medium and are the most prevalent of all types of TES. They work on the principle of thermal stratification which is based on the fact that the warmth and density of water are inversely proportional. This means that the warm water will always come to settle on top of the cold water and the interface between these two layers, which is the thermocline, will move up and down depending on whether the tank is being charged or discharged. Charging during the heating season means an increase in the quantity of hot water stored or equivalently the thermocline moving closer to the bottom of the storage tank.

Thus, it is evident that there are numerous thermal energy storage options that are available for coupling with the heat pump. However, irrespective of the choice of TES, a series combination of a heat pump and a TES can be modeled as a discrete-time first-order linear time-invariant system with additive uncertainty, as shown below:

$$E_{t+1} = aE_t + bu_t + w_t, \quad 0 \leq E_t \leq E_{max} \quad (3.1)$$

The state E (kWh) is the thermal energy stored in the tank. Each of the three TES models can be completely defined by E_{max} , the parameters a and b , and the disturbance w . It is assumed that the controlled variable u is compressor shaft speed in a vapor compression cycle. It is salient to note however that u can take on other values as well such as current flow through a resistive heating element or the heat flow provided to the storage device. Thus, the strength of the

formulation proposed above lies in its capability to capture the dynamics of different systems and therefore the control strategy that we develop in subsequent sections can be adapted for use with different types of thermal storage.

3.1.2 Thermal Energy Storage Model

To develop and test the model predictive control strategy which is the main focus of this research, a stratified thermal storage model is considered as it is the most widely used among all the TES devices mentioned earlier. Figure 3.2 illustrates this model and Table 3.1 defines the basic model parameters and exogenous input signals.

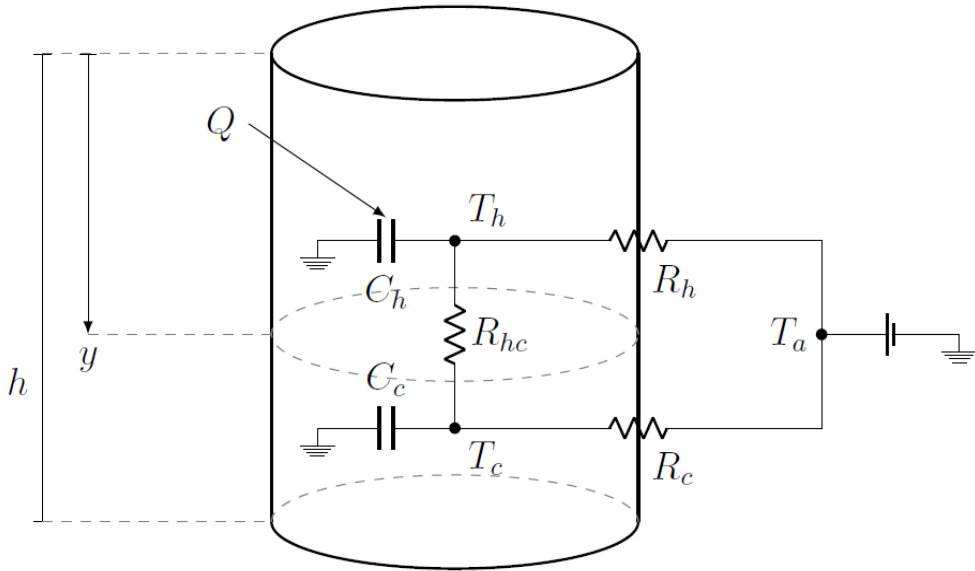


Figure 3.2: Schematic of the Stratified Thermal Storage System.

Table 3.1: Fundamental Model Parameters and Exogenous Input Signals

Quantity	Symbol	Units
Storage-ambient thermal resistance	R	$^{\circ}\text{C}/\text{kW}$
Storage thermal capacitance	C	$\text{kWh}/^{\circ}\text{C}$
Hot layer temperature	T_h	$^{\circ}\text{C}$
Cold layer temperature	T_c	$^{\circ}\text{C}$
Ambient temperature	T_a	$^{\circ}\text{C}$
Net heat flow injected to hot layer	Q	kW

Let us assume that the control systems inject a net heat flow Q into the hot layer; $-Q$ denotes heat extraction. Therefore, the thermal capacitance of the hot layer can be written as:

$$C_h = Cx \quad (3.2)$$

where, $x = y/h$, h is the tank height, y is the hot layer height and C is the combined thermal capacitance of the hot and cold layers. Similarly, the cold layer has capacitance:

$$C_c = C(1 - x) \quad (3.3)$$

The hot layer loses a heat flow

$$Q_{hc} = \frac{T_h - T_c}{R_{hc}} \quad (3.4)$$

to the cold layer through the contact resistance R_{hc} . The hot layer also loses a heat flow

$$Q_{ha} = \frac{T_h - T_a}{R_{ha}} \quad (3.5)$$

to the ambient through the effective resistance

$$R_{ha} = \frac{R}{x} \quad (3.6)$$

The capacitance C is defined as $C = \rho c_p V$, where ρ refers to storage material's density which in this case is water, c_p is its specific heat at constant pressure, and V is the tank volume. The thermal resistance R can be defined as $R = (1/h_- + l/k + 1/h_+)/A$. Here, h_- and h_+ are the convection coefficients at the inner and outer surfaces of the tank wall, l and k are the tank wall thickness and conductivity, and A is the wall surface area.

Similarly, the cold layer loses a heat flow

$$Q_{ca} = \frac{T_c - T_a}{R_{ca}} \quad (3.7)$$

to the ambient through an analogous effective resistance

$$R_{ca} = \frac{R}{1-x} \quad (3.8)$$

In deriving the above equations, it is assumed that the heat flow through the top and bottom surfaces of the tank is small compared to the heat lost through the tank wall.

Letting T_0 denote an arbitrary temperature at which the internal energy is defined to be 0, the internal energy of the hot and cold layers can be written as

$$\begin{aligned} E_h &= C_h(T_h - T_0) = C(T_h - T_0)x \\ E_c &= C_c(T_c - T_0) = C(T_c - T_0)(1-x) \end{aligned} \quad (3.9)$$

Thus, from the first law of thermodynamics, we have

$$\begin{aligned} \dot{E}_h &= Q - Q_{hc} - Q_{ha} \\ \dot{E}_c &= Q_{hc} - Q_{ca} \end{aligned} \quad (3.10)$$

In the above set of equations, \dot{E} represents the change in the internal energy over a time interval Δt . For simplicity, the value of the arbitrary temperature T_0 is taken as T_c which leads to $E_c = 0$ and $E = E_h$. Therefore, the total internal energy of the system can be written as:

$$E = C(T_h - T_c)x \quad (3.11)$$

The choice of T_0 also implies that $\dot{E}_c = 0$, so

$$Q_{hc} = Q_{ca} \quad (3.12)$$

Therefore, the storage dynamics can be written as:

$$\dot{E} = Q - Q_{ca} - Q_{ha} \quad (3.13)$$

The next step is to introduce the state E into the dynamics through the definitions of Q_{ha} , Q_{ca} , R_{ha} and R_{ca} . From the definition of E,

$$x = \frac{E}{C(T_h - T_c)} \quad (3.14)$$

Therefore,

$$\begin{aligned} \frac{1}{R_{ha}} &= \frac{x}{R} = \frac{E}{RC(T_h - T_c)} \\ \frac{1}{R_{ca}} &= \frac{1-x}{R} = \frac{1}{R} - \frac{E}{RC(T_h - T_c)} \end{aligned} \quad (3.15)$$

The total heat flow from storage to the ambient can therefore be written as

$$Q_{ha} + Q_{ca} = \frac{T_h - T_a}{R_{ha}} + \frac{T_c - T_a}{R_{ca}} \quad (3.16)$$

Substituting the values of R_{ha} and R_{ca} , we obtain

$$Q_{ha} + Q_{ca} = \frac{T_c - T_a}{R} + \frac{E}{RC} \quad (3.17)$$

Plugging this into Equation 3.13, we have

$$\dot{E} = Q - \frac{E}{RC} - \frac{T_c - T_a}{R} \quad (3.18)$$

It is evident that the stratified thermal storage model is a first-order linear time-invariant continuous time system,

$$\dot{E} = -E/\tau + Q + \nu, \quad 0 \leq E \leq E_{max} \quad (3.19)$$

where,

$$\tau = RC, \quad \nu = -\frac{T_c - T_a}{R}, \quad E_{max} = C(T_h - T_c) \quad (3.20)$$

Assuming that the heat flows and ambient temperature are constant over each time step, the model can be exactly discretized to

$$E_{t+1} = aE_t + bQ_t + w_t, \quad 0 \leq E_t \leq E_{max} \quad (3.21)$$

where,

$$a = e^{-\Delta t/\tau}, \quad b = -\tau(a - 1), \quad w_t = b\nu_t \quad (3.22)$$

The formulation of equation 3.21 conforms with the formulation that was stated earlier in equation 3.1.

3.1.3 Heat Pump Power Input and Thermal Output

The term Q in the previous sub-section is defined as the net heat flow injected into the hot layer and is basically the difference between the heat injected by the heat pump and the heat extracted by the downstream control systems to meet the space heating demand. In this section, a model describing the thermal output of the heat pump is obtained.

The actual dynamics of a variable speed heat pump (VSHP) are quite complex and they are generally described by coupled non linear differential equations as shown in [29] and [30]. Such models are not suitable for control purposes as they are computationally expensive and can also lead to non-convex

optimization formulations. Thus, simpler models are required that relate heat pump output and power consumption to variables such as ambient temperature and indoor temperature. The models developed by Kim et. al. [27] are suitable for our purpose. The authors use system identification techniques to come up with simple linear models for variable speed heat pumps that can be used in control applications.

$$\text{HP Power Consumption : } P_t = P(t) = \alpha_1 + \alpha_2 \cdot \omega(t) + \alpha_3 \cdot T_h + \alpha_4 \cdot T_a(t)$$

$$\text{HP Heat Output : } H_t = H(t) = \alpha_5 + \alpha_6 \cdot \omega(t) + \alpha_7 \cdot T_h + \alpha_8 \cdot T_a(t) \quad (3.23)$$

where, for a particular time instant t ,

$\omega(t)$ = Compressor Shaft Speed (rad/sec)

T_h = Temperature of the Hot Layer ($^{\circ}\text{C}$)

$T_a(t)$ = Ambient Temperature ($^{\circ}\text{C}$)

A crucial assumption made here is that the heat pump power consumption corresponds to power consumption by the compressor only and ignores the contribution by the fan. We make this assumption since compressor is the most energy intensive component of a heat pump.

Determination of Model Coefficients

To determine the value of coefficients for the equations above, we use performance data for Carrier's Infinity Series Variable Speed Heat Pump (Model: 25VNA024A) and fit linear regression models using least squares technique. As

per the product data sheet, the maximum rotational speed at which the compressor can operate during the heating mode is 5700 RPM (~ 600 rad/sec) and the lower limit is given as 1800 RPM (~ 190 rad/sec). The higher speed limit during the cooling mode is given as 3200 RPM (~ 335 rad/sec). The ambient temperature varies from -8°C to $+19^{\circ}\text{C}$ while the temperature of the space being heated or the condenser temperature varies from 18°C to 24°C . The manufacturer data is given specifically for 1800 and 3200 RPMs and we use this data to generate an input grid which is then used to fit the regression model. The values of the coefficients of the power and heat output equations obtained from this fitting process are shown in Table 3.2

Table 3.2: Coefficients of Fit for Pump Power Consumption and Thermal Output

Attribute	Coefficient	Value
Power	α_1	-0.5922
	α_2	0.0042
	α_3	0.0321
	α_4	-0.0023
Heat Output	α_5	-0.5091
	α_6	0.0203
	α_7	-0.0258
	α_8	0.1592

The regression coefficients obtained are in accordance with the operation of the heat pump as observed in the real world. The coefficient associated with condenser temperature in the heat pump power equation has a positive sign.

This means that for every one degree rise in the temperature of the space being heated, the pump power consumption increases by 0.0321 kW provided other factors are kept constant. At the same time, the heat energy output from the heat pump will decrease by 0.0258 kW as the coefficient associated with condenser temperature in the heat output equation has a negative sign. The cumulative effect of these results in a decrease in COP of the heat pump which is defined as ratio of heat energy output to the electrical power input to the heat pump. Similarly, we can also gauge the effect of varying the ambient temperature. A unit degree rise in ambient temperature will lead to decrease in heat pump power consumption by 0.0023 kW and an increase in heat output by 0.1592 kW. The cumulative effect of this is manifested as an increase in the COP. Both of these phenomenon are observed during the operation of heat pump in the real world. To estimate the quality of fit, the R-Squared value is computed for both the regression hyper-planes and these are shown in Table 3.3

Table 3.3: Regression R-Squared Values

Predicted Attribute	R-Squared Value
Power	0.996
Heat Output	0.994

The high R-Squared values indicate that the simple linear equations presented earlier adequately capture the performance of the VSHP and can be effectively used for developing the model predictive control strategy.

In this case, the space being heated corresponds to the hot layer in the stratified thermal storage and the fitted linear models are used to estimate the performance of the VSHP at higher storage temperatures and different compressor

shaft RPMs via extrapolation. The plots in Figure 3.3 show the heat pump performance characteristics that are obtained as a result of this extrapolation:

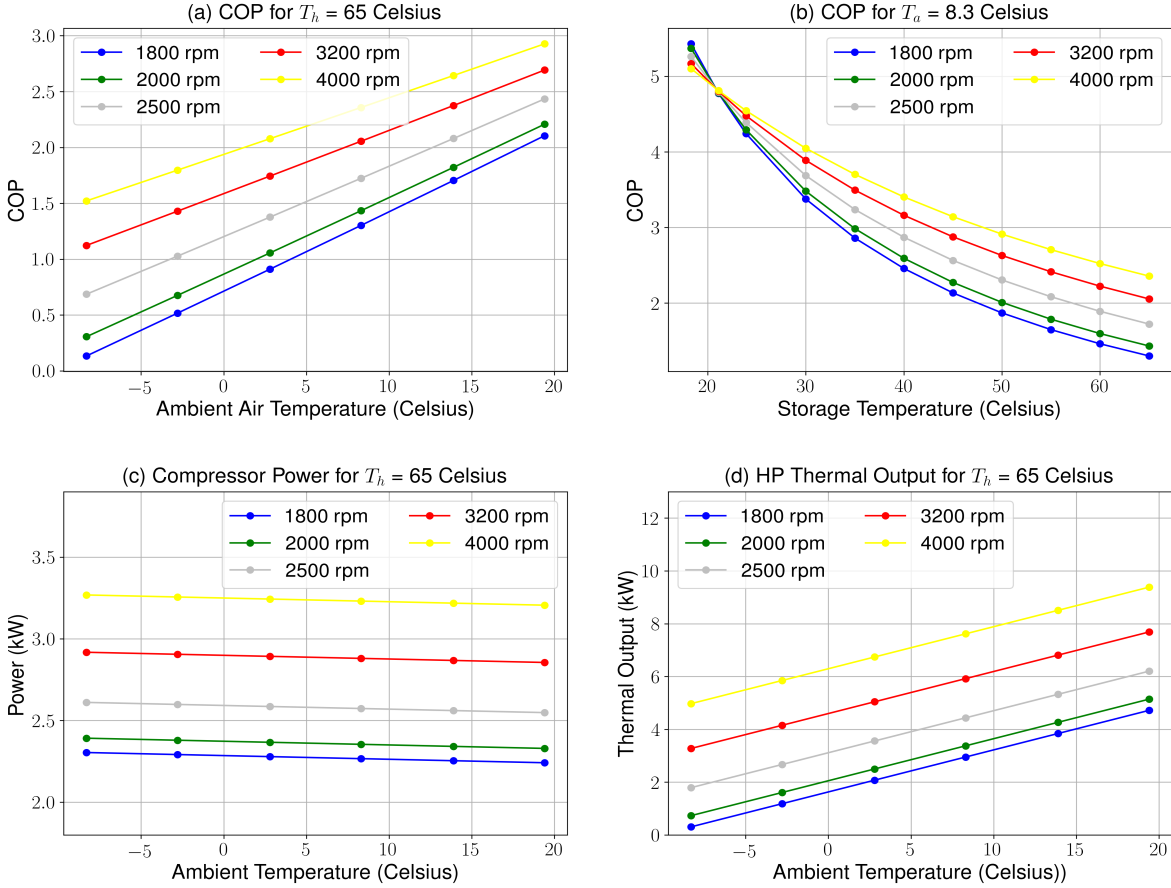


Figure 3.3: VSHP Performance Curves. Plot (a) shows that the heat pump COP increases with the increase in ambient temperature. Plot (b) shows the inverse relationship between COP and condenser temperature. Plots (c) and (d) show the variation of compressor power and heat pump thermal output with ambient temperature. The cumulative effect of these correspond to an increase in COP with increase in ambient temperature. These are in tandem with the operation of a heat pump in real world.

From the above plots, it is observed that the COP of the heat pump is decreases when the ambient temperature goes to negative or the temperature of

the thermal storage rises. Both of these events suggest that the heat pump has to work against a higher temperature gradient which leads to greater power consumption, thereby resulting in a lower coefficient of performance.

3.1.4 Space Heating Demand

As mentioned earlier, the other component of term Q in equation 3.18 pertains to the energy that is drawn from the thermal energy storage to meet the heating needs of the occupants. For the purpose of this research, instead of first principles modeling, we use DesignBuilder to come up with a daily profile of heating demand. DesignBuilder is a software tool that is used for the purpose of Building Performance Simulation (BPS). It provides an easy to use interface and docks to EnergyPlus for performing simulations. It also offers an extensive library of predefined building geometries and weather templates that can be used for performing simulations. Out of all the predefined geometries, we choose the International Energy Conservation Code's (IECC) Residential Prototype Low Rise Apartment as numerous heating systems in such large dwellings are ideal candidates for providing frequency regulation services. Figure 3.4 shows the rendered model of the building that is used.

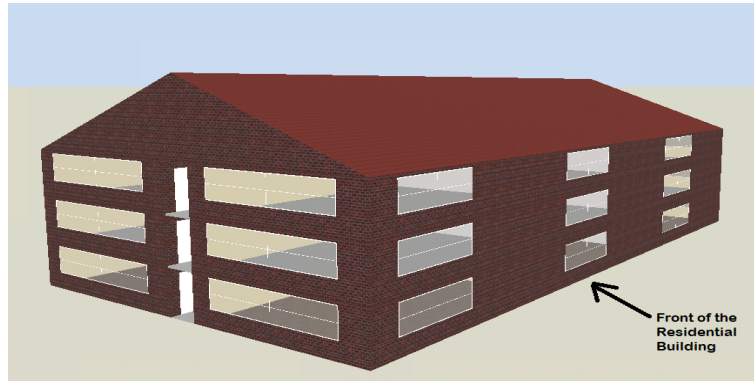


Figure 3.4: Rendered CAD Model of the Residential Low Rise Apartment. This prototype is simulated in EnergyPlus for obtaining the heating profile that is used in equation 3.18

There are 18 living units in the building and the thermal system caters to the heating needs of an individual unit. Out of all the units, the rightmost one situated on the bottom floor at the back of the building is considered since this unit will have a high heating requirement in comparison to units situated on the middle and the top floor. An important point to note here is that the heating demand can come from any type of accommodation. In other words, the control strategy that we develop can be used for any type of residence provided the dwelling derives heating from a heat pump.

3.2 Development of Model Predictive Controller

3.2.1 State Space Representation of the System

State space representation is a popular method of describing the dynamics of a physical system. For the purpose of this research, we use this type of repre-

sensation since the matrix form of the equation lends itself easily to the digital and analog computer methods of simulation. The general form of state space representation is given as:

$$x(t + 1) = A \cdot x(t) + B \cdot u(t) + C \cdot w(t) \quad (3.24)$$

In the above equation, $x(t)$ denotes the state of the system at time t , $u(t)$ represents the value of the manipulated variable at time t and $w(t)$ is the disturbance vector.

We start with the discretized equation 3.21 and replace the net heat flow injected term (Q) with the two components namely, the thermal output from the heat pump (H_t) and the space heating demand (Q_d). This yields the following equation

$$E_{t+1} = aE_t + b(H_t - Q_d) + \frac{b(T_a(t) - T_c)}{R} \quad (3.25)$$

We now substitute H_t with the formulation given in equation 3.23 and we obtain,

$$E_{t+1} = aE_t + b(\alpha_5 + \alpha_6 \cdot \omega(t) + \alpha_7 \cdot T_h + \alpha_8 \cdot T_a(t) - Q_d) + \frac{b(T_a(t) - T_c)}{R} \quad (3.26)$$

Additionally, a term specifying speed perturbation (\tilde{u}) from the fast local controller (refer to Figure 2.1) is also incorporated in the first principles equation. This cumulative speed perturbation originates as a result of the interaction between fast scale controllers during operation in the real time market. The magnitude of this signal is very small and this is modeled as a zero mean random Gaussian signal. This results in the following final discrete time formulation:

$$E_{t+1} = aE_t + b(\alpha_5 + \alpha_6 \cdot (\omega(t) + \tilde{u}) + \alpha_7 \cdot T_h + \alpha_8 \cdot T_a(t) - Q_d) + \frac{b(T_a(t) - T_c)}{R} \quad (3.27)$$

Thus, for the given control problem,

State Variable $x(t) = E(t)$

Manipulated Variable $u(t) = \omega(t)$

Disturbance Vector $w(t) = [1 \ T_a(t) \ Q_d \ \tilde{u}]^T$ (4 x 1 vector).

Therefore, the state space formulation of the discrete time equation takes the following final form:

$$x(t+1) = ax(t) + [\alpha_6 b] \cdot u(t) + \begin{bmatrix} (\alpha_5 + \alpha_7 T_h - T_c/R)b \\ b(\alpha_8 + 1/R) \\ -b \\ \alpha_6 b \end{bmatrix}^T \cdot \begin{bmatrix} 1 \\ T_a(t) \\ Q_d \\ \tilde{u} \end{bmatrix} \quad (3.28)$$

On comparing the above equation with equation 3.24, it is observed that A and B are scalar quantities while C is a 4 x 1 vector. The above formulation will be used to predict the dynamics of the system in model predictive control problem which is discussed in the next sections.

3.2.2 Performance Cost Modeling

The aim of MPC strategy is to come up with a control sequence such that both the cost of electricity associated with heat pump operation is minimized and the thermal comfort of the occupants is maintained. Additionally, the controller should ensure that deviations from reference power trajectory computed by the slow global controller are kept to a minimum. The objective or the cost function is formulated in a manner such that all of these requirements are reflected and addressed.

The energy cost associated with operation of heat pump can be written as:

$$g_e(t, x(t), u(t), w(t)) = \psi_e(t) \Delta t P(t) \quad (3.29)$$

where,

$$P(t) = \alpha_1 + \alpha_2 \cdot (\omega(t) + \tilde{u}) + \alpha_3 \cdot T_h + \alpha_4 \cdot T_a(t) \quad (3.30)$$

$P(t)$ is the electric power consumption of the heat pump at a particular time instant t . $\psi_e(t)$ are the utility's hourly Residential Time of Use (RTOU) electricity service rates ((\$/kWh) that are known in advance. Thus, for a 24 hour MPC simulation, these are known deterministically.

A stratified thermal storage can be charged to very high temperatures. This, in turn, will adversely affect the efficiency of heat pump as it will have to work against a larger temperature gradient and will also result in discomfort for the occupants. Therefore, an upper limit and lower limit to the amount of energy stored in the thermal storage is imposed. This constraint is encoded as a soft constraint into the objective function where variations beyond the upper and lower limits are penalized.

$$g_d(t, x(t)) = \psi_L(E_L - x(t))_+ + \psi_U(x(t) - E_U)_+ \quad (3.31)$$

Here, ψ_L and ψ_U (\$/kWh) are tunable, penalty parameters and the value of both is assumed as 0.3 \$/kWh. Moreover, the piecewise definition of the function $f: (g)_+$ is:

$$f = \begin{cases} g, & \text{if } g \geq 0 \\ 0, & \text{if } g < 0 \end{cases}$$

Encoding the upper and lower energy storage limits as soft constraints introduces greater flexibility in the operation of the system as minor variations beyond the limits are allowed. This would not be the case if the limits were encoded as hard constraints in the optimization problem.

Therefore, the net stage cost (objective function) is given as:

$$g_k(x(t), u(t), w(t)) = g_e(t, x(t), u(t), w(t)) + g_d(t, x(t)) \quad (3.32)$$

The solution of the optimization problem with equation 3.32 as the objective function will yield the initial power trajectory and this will be sent to the slow global controller operating at the entire building level. The global controller receives many such power trajectories from different MPC controllers and solves a distributed convex optimization after taking into account the frequency regulation signal sent by the system operator. This results in a new power trajectory that needs to be followed by the heat pump/thermal storage subsystem. To ensure this, an additional cost term is appended to the stage cost to reflect the need to follow the reference power trajectory.

$$g_p(t, x(t), u(t), w(t)) = \rho(\|P(t) - \hat{P}\|_2)^2 \quad (3.33)$$

Therefore the net stage cost in this scenario can be written as:

$$g_k(x(t), u(t), w(t)) = g_e(t, x(t), u(t), w(t)) + g_d(t, x(t)) + g_p(t, x(t), u(t), w(t)) \quad (3.34)$$

With this augmented objective function, the MPC algorithm is run again and a new pump power sequence is obtained which is communicated to the higher level controllers.

3.2.3 Open-Loop Optimal Control Problem

Given an initial state x_0 , the total expected cost of a sequence of control inputs $\pi = \{u(0), \dots, u(N-1)\}$ is,

$$J_\pi(x_0) = \mathbf{E} \sum_{t=0}^{N-1} [g_k(x(t), u(t), w(t))] \quad (3.35)$$

Therefore, the stochastic optimal control problem can be formulated as,

$$\text{minimize } J_{\pi}(x_0) \quad (3.36)$$

subject to

$$x_{t+1} = ax_t + (\alpha_5 + \alpha_6 \cdot \tilde{u} + \alpha_7 \cdot T_h + \alpha_8 \cdot T_a(t))b \cdot y(t) + \alpha_6 \cdot u(t) \cdot b - Q_d b + \frac{b(T_a(t) - T_c)}{R} \quad (3.37)$$

$$190y(t) \leq u(t) \leq 600y(t) \quad (3.38)$$

$$y(t) = 0, 1[\text{Binary Variable}] \quad (3.39)$$

where the constraints apply for all $t \in \{0, \dots, N - 1\}$.

In the objective function above, $N = (T/\Delta t)$ refers to the number of discrete time steps of length Δt (hours) in the control horizon T and $P(t)$ is written as:

$$P(t) = (\alpha_1 + \alpha_2 \cdot \tilde{u} + \alpha_3 \cdot T_h + \alpha_4 \cdot T_a(t))y(t) + \alpha_2 \cdot u(t) \quad (3.40)$$

It should be noted that the problem is formulated as a mixed integer linear program with the binary variable $y(t)$. This is done to simulate the performance of a variable speed heat pump in the real world. A value of $y(t) = 0$ signifies that the heat pump is switched off and a value of $y(t) = 1$ signifies that the heat pump is in operation at a particular time step t . Additionally, when the heat pump is in operation, the compressor speed will vary between 190 to 600 rad/sec depending on the solution of optimization problem.

CHAPTER 4
SIMULATION RESULTS & DISCUSSION

The residential prototype low rise apartment building (presented in §3.1.4) is assumed to be located in the Central Region [31] of New York State. Additionally, the value of the time invariant parameters is shown in Table 4.1

Table 4.1: Time Invariant Simulation Parameter Values

Quantity	Units	Value
Control duration, T	hours	24
Time step, δt	hours	1
MPC Horizon, H	-	24
Storage tank volume, V	m^3	2.567
Storage thermal capacitance, C	kWh/°C	2.975
Storage-ambient thermal resistance, R	°C/kW	438.86
Hot layer temperature, T_h	°C	65
Cold layer temperature, T_c	°C	50
TES Lower Energy Limit, E_L	kWh	0
TES Upper Energy Limit, E_U	kWh	45

To analyze the performance of developed controller under a variety of temperature and heating load conditions, 100 Monte Carlo runs are performed using simulation data from DesignBuilder. Each day starting from December 1st, 2002 to March 10th, 2003 is treated as a candidate for Monte Carlo run. To obtain the space heating profile of the living unit situated on the ground floor, the

building prototype is simulated with occupancy, lighting and plug load schedules obtained from the inbuilt 'residential_schedule' template. This simulation yields the living unit's hourly heating demand for the entire winter season from November 1st, 2002 to March 31st, 2003. The hot and the cold layer temperatures are decided such that the temperature of the water is optimal for the purpose of space heating. Additionally, the upper limit to the thermal energy storage is ascertained by solving an open loop optimal control problem (OLOC) for the coldest day in the data set. In OLOC, perfect forecasts of temperature and heating load are assumed and the optimization problem is solved such that the states and controls are obtained for all the time steps in a single run. It is also important to note here that setting the MPC time step to a large value (in this case $\delta t = 1$ hour) enables us to focus solely on the steady state characteristics of the heat pump. For higher frequency control purposes, the transient characteristics should also be considered.

From equation 3.28, it is evident that for making thermal storage state predictions at successive time steps, predictions of ambient temperature and space heating load are required. A number of studies assume perfect forecasts for such exogenous disturbances. This assumption, even though resulting in a good control strategy, is not applicable in a real world scenario. Thus, for ensuring that an optimal control strategy is obtained, accurate predictions of the exogenous disturbances, which in this case comprise of ambient temperature and living unit's heating load are required.

For predicting the ambient temperature, we use a seasonal auto regressive integrated moving average (SARIMA) model as its predictive accuracy is well established for univariate time analysis. A seasonal auto regressive model is

used as opposed to a normal auto regressive model as there is a strong daily seasonal trend associated with the temperature data as depicted in Figure 4.1. Using Dickey-Fuller test, it is ascertained that taking the first difference of the univariate time series makes the data stationary.

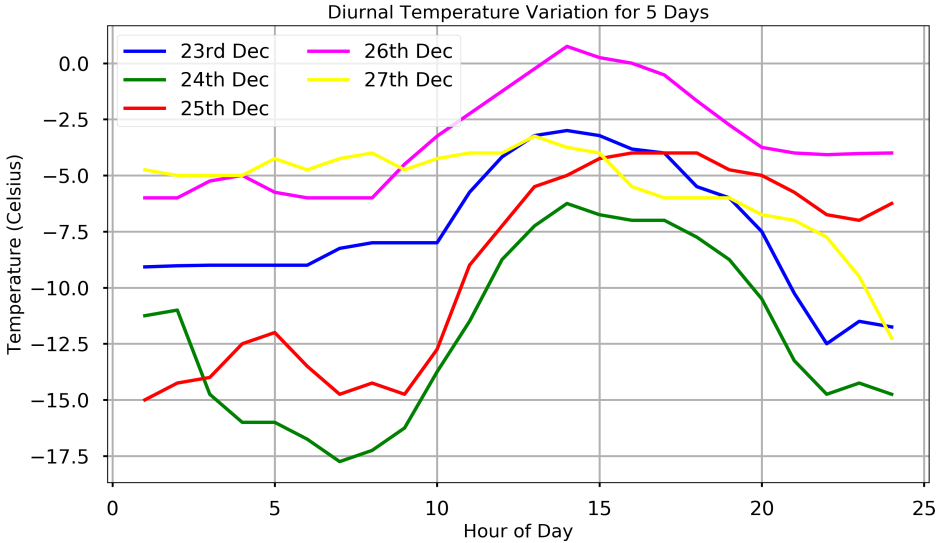


Figure 4.1: Diurnal Trend of Non-Stationary Temperature Data. The similar shapes of temperature profiles for 5 days suggest the presence of daily seasonality which makes the data non-stationary. This suggests that ARIMA models coupled with data differencing techniques or in other words SARIMA models need to be used for making diurnal temperature predictions.

Using the auto correlation and partial auto correlation functions, the number of auto regressive (AR) and moving average (MA) terms are determined to be 1. Thus, the final order of the SARIMA model used is $(1, 1, 1)(1, 1, 1)_{24}$ where, in the first tuple, the first term denotes the order of the AR model, second term denotes the degree of differencing and the third term denotes the order of the moving average model. The three terms in the second tuple also have a similar interpretation with the only difference being that they are associated with the

seasonal part of the ARIMA model. The number 24 corresponds to number of periods in each season which in this case is a single day.

For predicting the heating load, we analyze the performance of SARIMAX and Random Forest methods. Based on the quality of predictions, we decide to go ahead with the latter. It is an ensemble learning technique that combines many decision trees to come up with a strong regressor. The input space for the random forest model is comprised of the hour of the day and the ambient temperature since it is negatively correlated with the heating load. We train the model using the entire data set for the month of November. The first step involves determining the optimal value of the model hyper parameter which in this case is the number of decision trees that are used as estimators. A 5-fold cross validation approach is used for this purpose and the optimal value of the hyper parameter is determined to be 5 as depicted by Figure 4.2.

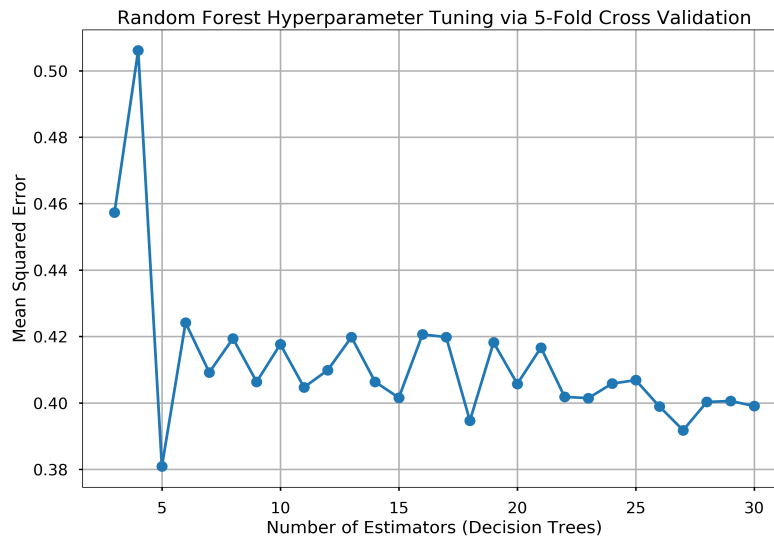


Figure 4.2: Hyper parameter Tuning for Random Forest. This shows the results of 5-fold cross validation used for determining the optimal number of decision trees

The aforementioned models are then used for making predictions at an hourly interval for the next 100 days with the output of the SARIMA model being used by the Random Forest Model for making heating demand predictions. Figure 4.3 shows the performance of both these models in predicting the daily temperature and space heating demand for the 100 day span. The data from DesignBuilder is assumed to be the true value of the quantities being predicted. Both the models have relatively high accuracy with the SARIMA model having better performance than the random forest model. There are some bad predictions in case of both the models and the performance of the MPC controller will be adversely affected on these days.

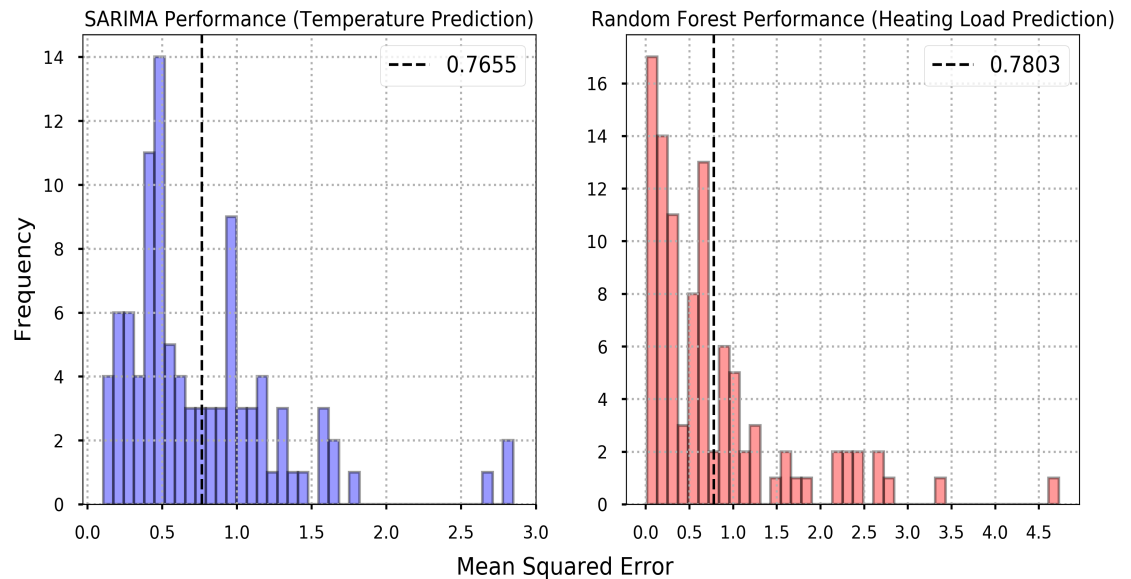


Figure 4.3: Predictive Performance of SARIMA and Random Forest Models. These plots give an estimate of the performance of algorithms used for making diurnal temperature and heating load predictions for 100 Monte Carlo Simulations. The dotted vertical lines in the plots denote the mean of the plotted values.

4.1 Value of Mixed Integer Approach

As mentioned earlier, the MPC optimization problem is formulated as a mixed integer program so that the problem of heat pump operation in compressor dead-band can be addressed and at the same time ensure when the compressor is turned off, the power consumption and thermal output from the heat pump become zero. In this section of results, it is assumed that the controller is operating in the stand alone mode with no interfacing to the global controller. Thus, the objective of the MPC controller is to minimize the energy costs while ensuring that the thermal comfort of the occupants is maintained. Another important point to note here is that the optimization problem formulated in the previous section is essentially a Mixed Integer Quadratic problem. If we remove the tracking term, we end up with a Mixed Integer Linear Program. Both these formulations can easily be solved by available solvers. For the purpose of this research, the optimization runs are done in CVX [32] using Gurobi [33] as the solver instead of SDPT3. This switch is performed since Gurobi is capable of performing Mixed Integer programming unlike SDPT3.

The entire system is analyzed under New York State Electric and Gas Corporation's (NYSEG) three tiered residential time-of-use electricity service rate [34] and a 24 hour MPC problem is solved at hourly time steps.

The performance of the developed controller is also shown for a typical day and Figure 4.4 shows the true and the predicted values of the exogenous disturbances for the selected simulation day.

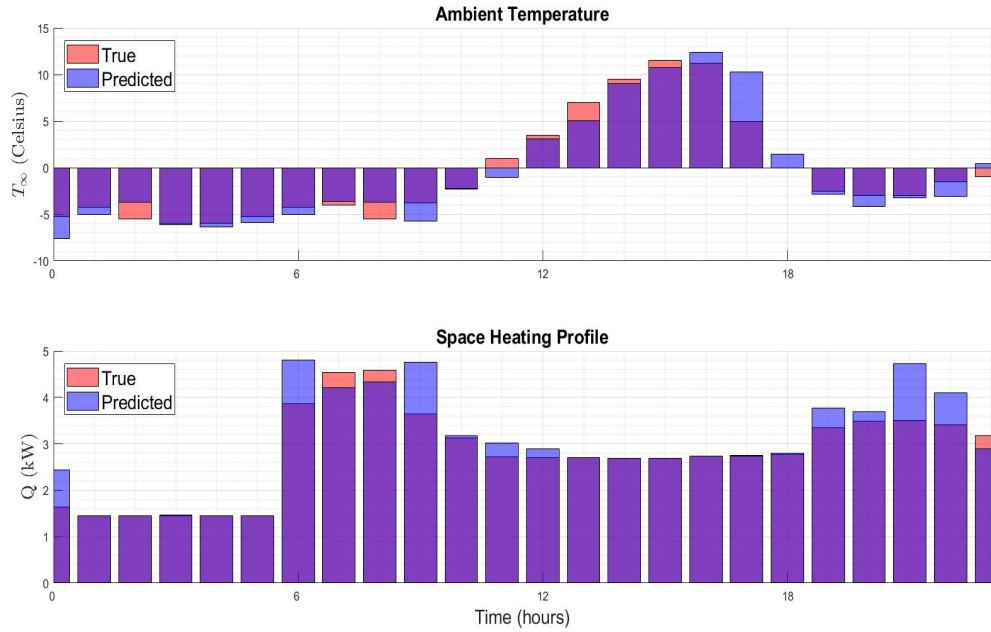


Figure 4.4: True and Predicted Values of the Exogenous Disturbances. The top plot shows the predicted and true values of the ambient temperature for the simulation day. The bottom plot does the same for heating load. The predicted values are used for making state predictions in the MPC horizon while the true values are used for updating the system state at each MPC iteration. With a mean square error of 0.67 for temperature predictions and 0.165 for heating load predictions, the quality of predictions is good. This fact is crucial as good predictions ensure that the control policy obtained is optimal. Bad predictions can lead to sub-optimal control policies with high system operating costs.

As mentioned earlier, an OLOC problem involves solving a certainty equivalence problem with the assumption of perfect forecasts of exogenous disturbances. This helps in establishing a lower bound on the cost of daily operations and this mode of control is termed as prescient control. It is important to note that the control policy obtained from this algorithm cannot be implemented as it is not causal. The system states and controls obtained under the MPC and

prescient control regimes are shown in Figure 4.5.

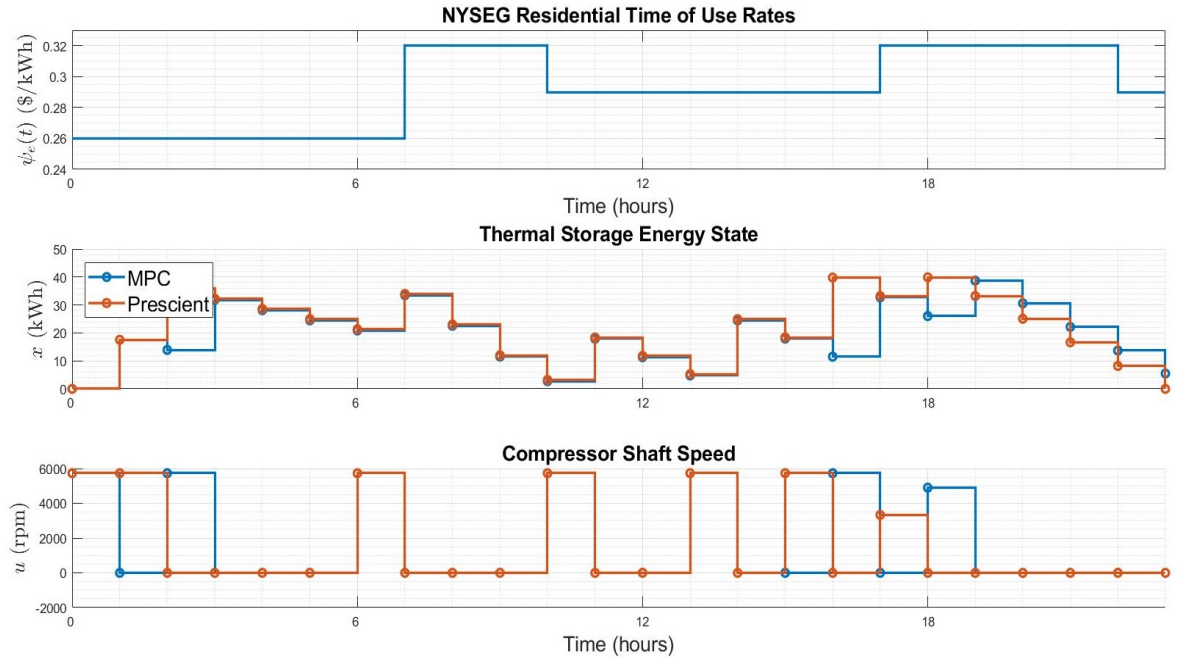


Figure 4.5: System States and Controls Under the MPC and Prescient Policy. The first plot shows NYSEG’s three tiered i.e. off-peak, on-peak and mid-peak electricity service rate. For plots 2 and 3, the baseline (shown in orange) is computed by solving a certainty equivalence problem and provides a lower bound on the performance of the MPC algorithm. Furthermore, it is observed that the thermal storage is charged during the time of low electricity prices and is ultimately used during the time of high energy prices to meet the heating needs.

It is observed that, in both the cases, the heat pump is used to charge the thermal storage during the time of off-peak prices. As soon as the on-peak price sets in, the heat pumps are turned off and the heating needs of the living unit are met entirely by the thermal storage. Such a system is capable of participating directly in the electricity market as the RTOU price structure can be replaced by price signals sent by the power system operator.

To ascertain the value of mixed integer formulation, the performance of MPC framework using this formulation is compared against a formulation that involves no binary variables and uses the heat pump performance models as proposed by Kim et. al. Under this condition, the latter formulation involves solving a simple linear program. Figure 4.6 show the system states and controls under both the formulations. It is observed that the simple linear formulation allows operation in the compressor dead-band (0 - 1800 RPM) as shown by operating points lying in the shaded area. The mixed integer formulation overcomes this issue, thereby proving its efficacy.

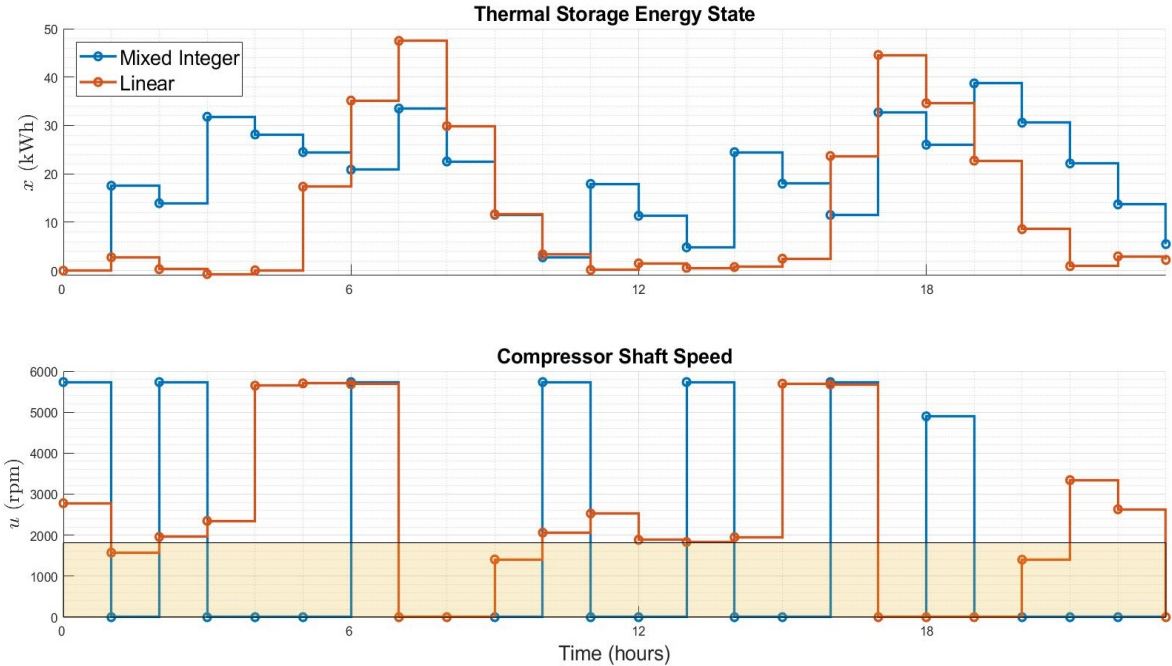


Figure 4.6: System States and Controls Under Mixed Integer and Simple Linear Formulation. The shaded area in the second plot denotes operation in the compressor dead-band as suggested by using the original heat pump performance equations. This issue is adequately addressed by the introduction of binary variables which enable the model avoid operation in the compressor dead band.

The other advantage of introducing binary variables in the formulation is that they overcome the anomalous behavior of heat pump performance equations which originally suggest that the heat pump will consume power and produce heat at zero compressor shaft speeds. This is illustrated in figure 4.7

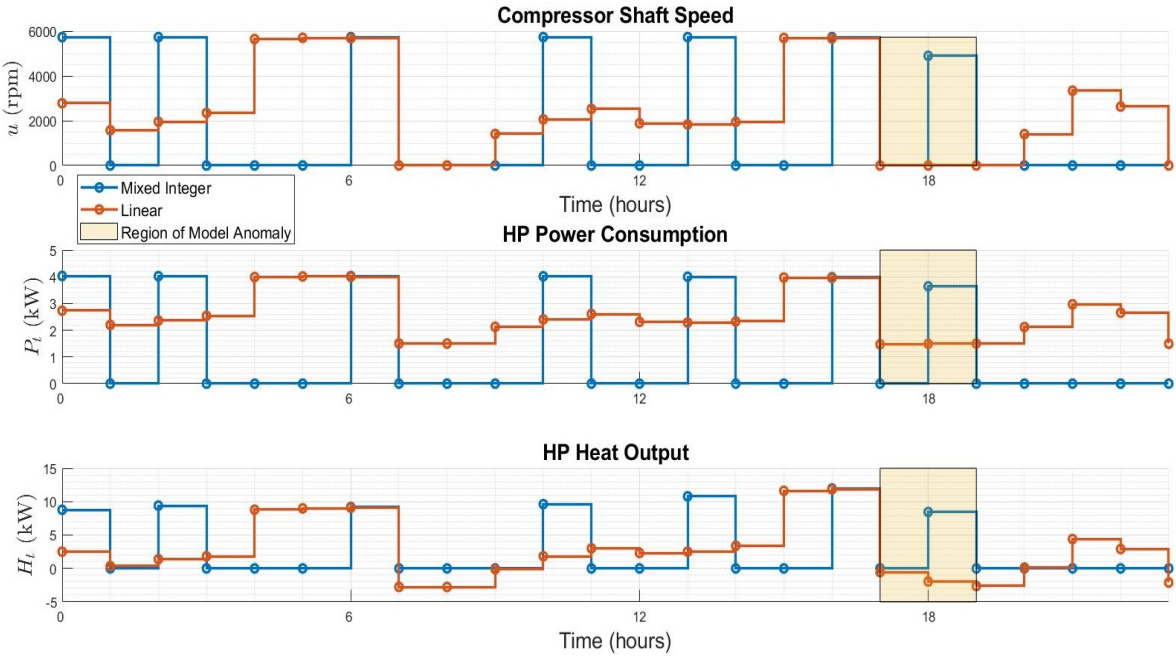


Figure 4.7: Comparison of Heat Pump Power Consumption and Thermal Output Under Mixed Integer and Simple Linear Formulation. The shaded areas in the plots highlight the anomaly associated with using the original heat pump performance models as non-zero power consumption and heat output values are obtained at zero compressor shaft speeds. On the other hand, the mixed integer formulation rectifies this anomaly and drives the pump power consumption and heat output to zero at zero compressor speeds.

Additionally, the increase in running time associated with formulating the optimization problem as a mixed integer as opposed to simple linear is not significant. This is evident from figure 4.8 in which simulation runtimes are plotted

for 100 Monte Carlo runs of the system when operating under the mixed integer and linear formulations.

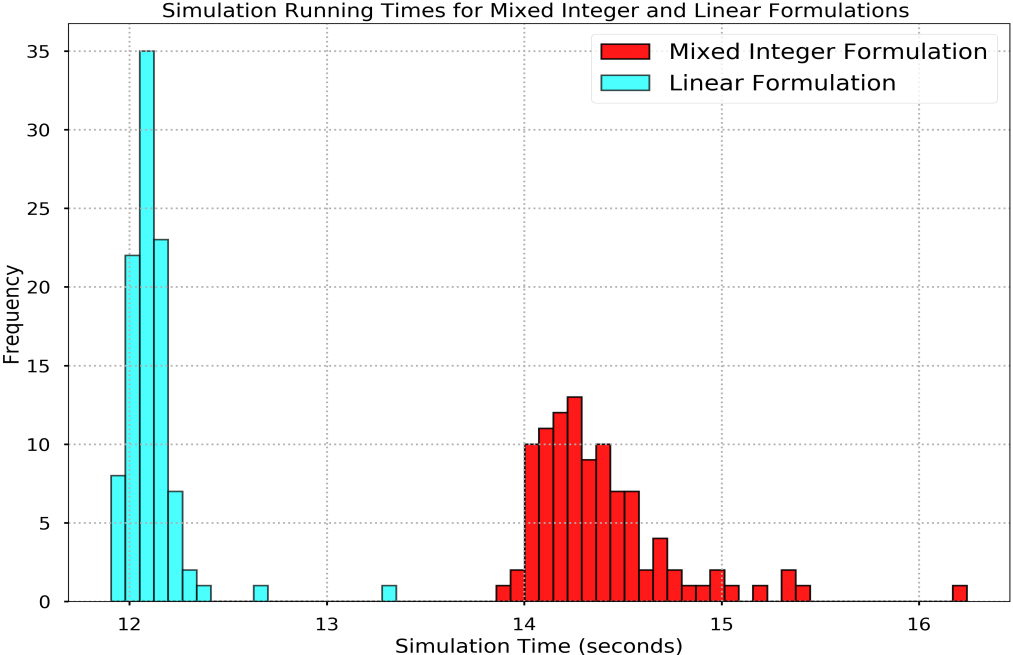


Figure 4.8: Simulation Run Times for Mixed Integer and Simple Linear Formulation. The average run time for mixed integer formulation (14.4 seconds) is slightly greater than that of the linear formulation (12.1 seconds). Thus, the mixed integer formulation can easily be implemented without incurring a significant increase in processing time.

Figure 4.9 shows the number of compressor dead band violations plotted against the Monte Carlo run when the optimization problem is solved without the use of binary variables to augment the heat pump performance models. These require a post processing step which is eliminated by adopting a mixed integer approach.

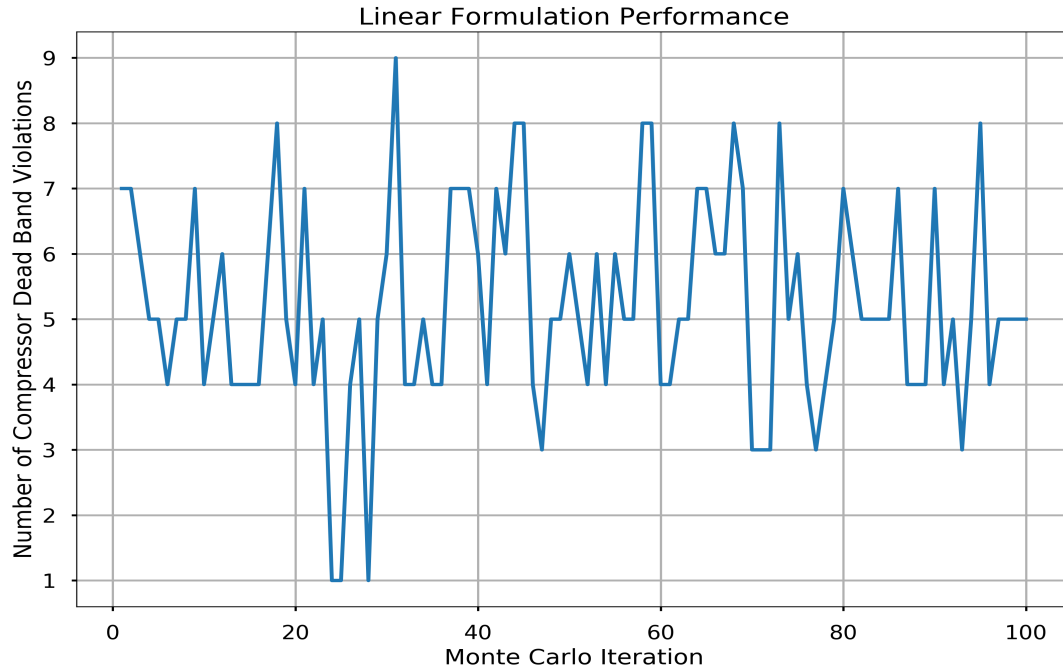


Figure 4.9: Frequency of Compressor Dead Band Violations under Linear Formulation. The above plot shows the number of control points, as computed by solving the linear formulation, that lie in the compressor dead band range for each Monte Carlo iteration. [1] and [2] tackle this problem by implementing a post-processing step as discussed earlier. Having a mixed integer formulation essentially eliminates this post-processing step.

4.2 Power Tracking Performance of MPC Controller

The interfaced operation of the MPC controller introduces an additional objective into the framework which pertains to tracking of the power sequence sent by the higher level controller. Thus, the MPC problem needs to be resolved in the presence of dual objectives of minimizing energy cost and tracking the reference power sequence with minimal deviations. To simulate this scenario, two inputs from the higher level controller are required: value of the penalty

parameter ρ and the 24 hour reference power trajectory on an hourly time scale (Refer to equation 3.33). In the absence of the higher level controller, we come up with a hypothetical scenario where it is assumed that the goal of higher level controller is to maximize the revenue from providing frequency regulation service. This decision is driven by the fact that frequency regulation is considered as the most lucrative service in the electricity market. Thus, to maximize revenue, the higher level controller should have maximum flexibility available at its disposal. The controller can procure this flexibility by ensuring that an individual heat pump/thermal energy storage subsystem's power consumption is in the middle of its upper and lower limits. This, in turn, would ensure that the subsystem has maximum upward and downward flexibility. This assumption gives us the hypothetical constant reference power trajectory that can be expected from the higher level controller. The value of the penalty parameter ρ is also obtained from higher level controller and we examine the power tracking performance of the algorithm under different values of this parameters. The results for the same are shown in Figure 4.10.

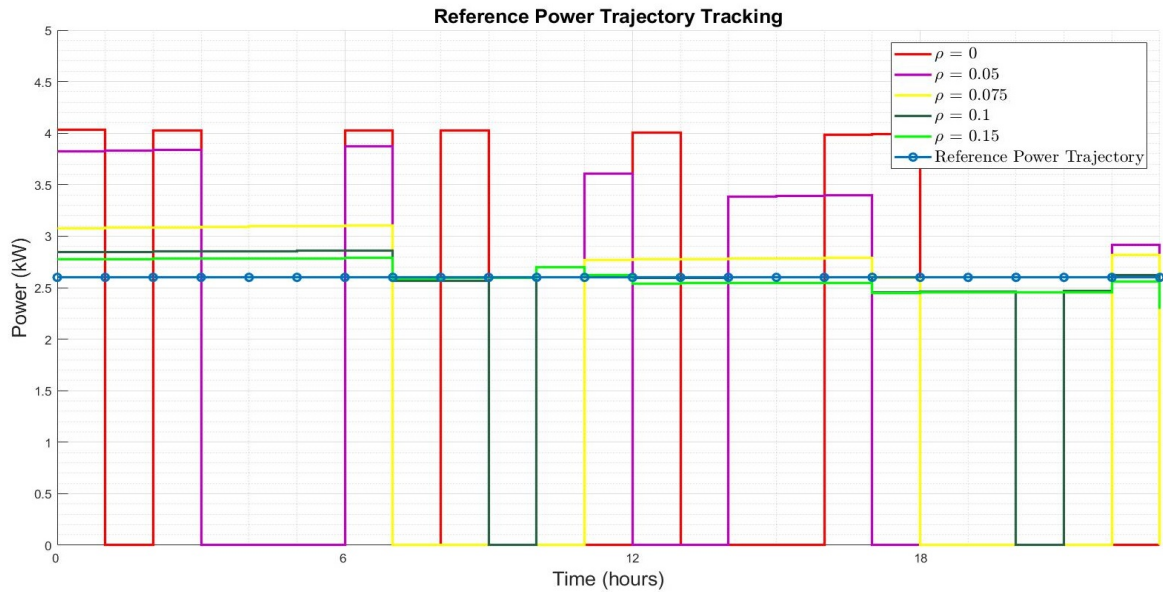


Figure 4.10: Tracking Performance of MPC Controller. This plot shows the pump power profiles for different values of the penalty parameter ρ . It is observed that as the value of the tunable parameter increases, the subsystem level controller forces the pump power sequence to inch closer to the reference power trajectory. This behavior proves the effectiveness of MPC framework to closely track the reference power signal from higher level controllers, thereby ensuring that the subsystem can participate in the frequency regulation market.

It is observed that as the value of the penalty parameter increases, the pump power profile inches closer to the reference power trajectory and for very large values can exactly track the reference trajectory. Thus, the tracking viability of the developed controller is proven.

CHAPTER 5

CONCLUSION

In this work, a model based predictive control strategy is developed that facilitates the integration of a heat pump/thermal storage subsystem into a hierarchical control architecture for the purpose of participating in the frequency regulation market. The developed MPC controller operates in two modes to achieve this. The first mode involves stand alone operation where the MPC controller computes a trajectory of control inputs to the compressor of the variable speed heat pump such that the energy costs associated with the operation of the system are minimized. One of the contributions of this study pertains to the use of mixed integer programming to improve the MPC design for this mode of operation. Introducing binary variables in the optimization framework enables us to adequately address the problem of preventing operation in the dead-band of the heat pump compressor as indicated by Figure 4.6. An additional advantage of using this formulation is that it increases the general applicability of simple, yet comprehensive, heat pump performance models as the same models can now be effectively used in scenarios when the heat pump's compressor is turned off. This aspect is shown in 4.7 where anomalous associated with using original heat pump performance models in a linear formulation is overcome by introducing binary variables in the fray. In the process, the overall performance of the model predictive controller is also increased. Another salient aspect is the use of machine learning techniques, namely SARIMA and Random Forest, for the prediction of exogenous disturbances as opposed to some studies that assume perfect knowledge of such parameters.

The second mode involves the interfaced operation of MPC controller within

the global control architecture. To achieve this, the MPC framework is extended to include an additional objective which pertains to tracking of a power sequence for the purpose of frequency regulation. This additional objective is encoded as the square of the Euclidean norm of a vector whose elements denote the deviation between the pump power sequence and the reference power trajectory. This term is multiplied by a penalty parameter which is also obtained from the higher level controller and the term is appended to the objective function. This essentially converts the problem to a Mixed Integer Quadratic program. Resolving the optimization problem for different values of the penalty parameter shows the effectiveness of the MPC algorithm in tracking the power signal from higher level controller amidst other competing objectives. Thus, the development of such a framework where the low level controller is capable of effectively responding to signals from a higher level controller forms the second contribution of this work.

There are many possible extensions to the current work. The most obvious one is the proper sizing of thermal storage. For this work, the thermal storage was sized on the basis of heating requirement on the coldest day. This is certainly not the most optimal way of sizing and thus future work can focus on conducting a sensitivity analysis following which the objective function of the optimization framework can be extended to simultaneously decide the optimal size of thermal storage. Future work can also focus on analyzing the effects of coupling different types of thermal storage with the heat pump such as phase change thermal storage. The MPC strategy developed in this work encodes the thermal energy stored in the storage as a state variable and can thus facilitate the analysis of different types of thermal storage. Another possible area of future work can be focused on analyzing different formulations that can be used for

imposing the reference power trajectory constraint. This work focused only on the Euclidean norm and other norms such as Absolute-Value norm or Manhattan norm can also be looked into. This work assumed that the heat pump and thermal storage are connected in a series configuration. However, the mixed integer programming approach can be extended to simulate a parallel configuration and this can form the basis of a future research. Finally, while the MPC algorithm presented in this work appears to work as per our expectations, it might not necessarily be the best one. Thus, future work can be directed towards implementing different algorithms which might more closely approximate the optimal causal policy.

APPENDIX A

ELEMENTS OF MODEL PREDICTIVE CONTROL

As with many effective control strategies, predictive control has its origin in human behavior as well. Predictions are involuntarily used by humans to understand the behavior of the world around them. As an example, in chess, a good player predicts the game a few steps ahead based on the moves of the opponent and plans a few future moves. However only one move can be implemented at each time. Based on the next move of the opponent a new set of predictions has to be made and a new set of future moves is determined as a result. The goal of predictive control is to automate this decision making process using a computer.

Any model predictive control law contains the basic components of prediction, optimization and receding horizon strategy [18]. A given model that will describe the dynamics of the system is paramount in predictive control. A good dynamic model will give a consistent and accurate prediction of the future. This system model is required by MPC to minimize the difference between the predicted output and the desired output. The system model used could be either physical or empirical and linear or non linear. Typically a linear empirical model is used. Some typical linear models used are step response models, transfer function models, and state space models.

The next important component of the predictive strategy is online optimization. The predictive control feedback law is computed by minimizing a performance cost which is defined in terms of the predicted sequence x and u . This objective function is often called the cost function and can take a quadratic or linear form. Most of the MPC problems have quadratic cost functions which lie

in the domain of disciplined convex optimization. Solving such formulations ensure that the solution that is arrived at is a global optimum rather than a local optimum. Such optimization problems generally have constraints which are used to represent limitations on system components that arise from physical, safety or economic constraints.

Receding horizon implementation forms the third ingredient of MPC. The optimization is carried out over a certain time window called the prediction horizon. This dictates how 'far' the future states of the controlled be predicted. This parameter equals the length of the moving horizon window which is the time-dependent window from an arbitrary time t_i to $t_i + T_p$. The length of this window remains constant. Therefore, outputs are calculated at each interval in the horizon based on values at time t and these are sent to the controller. Although the optimal trajectory of future control signal is completely described within the moving horizon window, the actual control input to the plant only takes the first sample of the control signal while neglecting the rest of the trajectory. This is because the control law has access to new state and disturbance measurements that can be used for updating the string of input signals in the prediction horizon. This is evident in Figure A.1 where we observe two different control sequences at time k and at $k+1$.

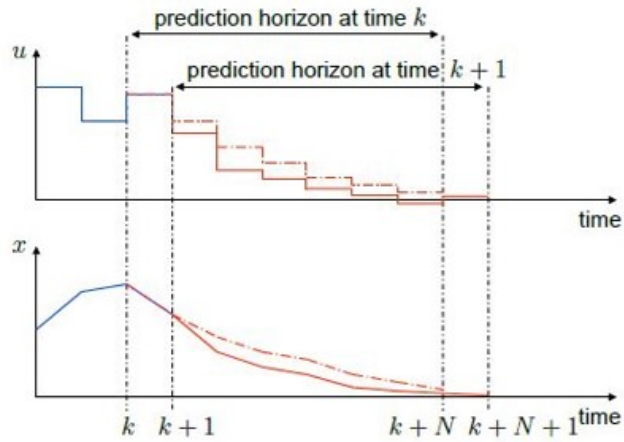


Figure A.1: Receding Horizon Implementation

It is important to note that the length of the prediction horizon remains same. Since the current state of the system is used at each time step to compute the control sequence, feedback is introduced into the MPC law, thereby ensuring system robustness against modeling errors and uncertainty. The receding horizon implementation also compensates for the fact that the moving window is finite. Figure A.2 summarizes the working of MPC algorithm.

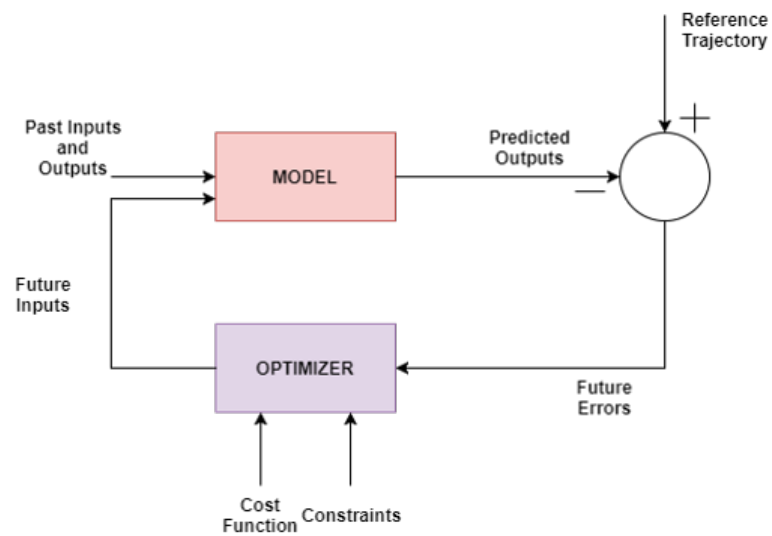


Figure A.2: Model Predictive Control Algorithm

REFERENCES

- [1] Clara Verhelst, Filip Logist, Jan Van Impe, Lieve Helsen, "Study of the Optimal Control Problem Formulation for Modulating Air-to-Water Heat Pumps Connected to a Residential Floor Heating System," *Energy and Buildings*, vol. 45, pp. 43–53, 2012, ISSN 0378-7788.
- [2] N. Saraf, "Predictive Control for Residential Capacity Controlled Heat Pumps in a Smart Grid Scenario," M.S. thesis, Delft University of Technology, 2015.
- [3] US Energy Information Administration, "Residential Energy Consumption Survey," https://www.eia.gov/consumption/residential/reports/2009/state_briefs/, 2013.
- [4] Inspectapedia, "Gas Furnaces and Indoor Air Quality," https://inspectapedia.com/Environment/Gas_Furnace_IAQ.php.
- [5] Office of Energy Efficiency, Natural Resources Canada, "Heating and Cooling with a Heat Pump - EnerGuide," .
- [6] Nordic Heating & Cooling, "Do Air Source Heat Pumps Work in Cold Climates," <https://www.nordicghp.com/2015/12/air-source-heats-pump-cold-climates/>.
- [7] Zhaoxi Liu, Qiuwei Wu, A. H. Nielsen, J. Østergaard and Yi Ding, "Electricity Demand Profile With High Penetration of Heat Pumps in Nordic Area," *2013 IEEE Power & Energy Society General Meeting*, pp. 1–5, 2013, doi: 10.1109/PESMG.2013.6672924.
- [8] Fawcett, Tina & Eyre, Nick & Layberry, Russell, "Heat Pumps and Global Residential Heating," 2015.
- [9] S. J. G. Cooper, G. P. Hammond, M. C. McManus and D. Pudjianto, "Detailed Simulation of Electrical Demands Due to Nationwide Adoption of Heat Pumps, Taking Account of Renewable Generation and Mitigation," *IET Renewable Power Generation*, vol. 10, no. 3, pp. 380–387, 2016, doi: 10.1049/iet-rpg.2015.0127.
- [10] R. Renaldi, A. Kiprakis, D. Friedrich, "An Optimisation Framework for Thermal Energy Storage Integration in a Residential Heat Pump Heating

- System," *Applied Energy*, vol. 186, no. 3, pp. 520–529, 2017, ISSN 0306-2619, <https://doi.org/10.1016/j.apenergy.2016.02.067>.
- [11] Armada Power, "What is Frequency Regulation?," <https://www.armadapower.com/frequency-regulation.html>.
- [12] M. Waite, V. Modi, "Potential for Increased Wind-Generated Electricity Utilization Using Heat Pumps in Urban Areas," *Applied Energy*, vol. 135, pp. 634–642, 2014, ISSN 0306-2619.
- [13] E. Georges, S. Quoilin, S. Mathieu, V. Lemort, "Aggregation of Flexible Domestic Heat Pumps for the Provision of Reserve in Power Systems," University of Liege, Belgium, <https://hdl.handle.net/2268/212788>.
- [14] M.T. Muhssin, L.M. Cipcigan, N. Jenkins, S. Slater, M. Cheng, Z.A. Obaid, "Dynamic Frequency Response from Controlled Domestic Heat Pumps," *IEEE Transaction on Power Systems*, DOI 10.1109/TPWRS.2017.2789205.
- [15] Hedegaard, K, Mathiesen, BV, Lund, H & Heiselberg, "Wind Power Integration Using Individual Heat Pumps Analysis of Different Heat Storage Options," *Energy*, vol. 47, pp. 284–293, 2012, DOI: 10.1016/j.energy.2012.09.030.
- [16] David Fischer, Hatef Madani, "On Heat Pumps in Smart Grids: A Review," *Renewable and Sustainable Energy Reviews*, vol. 70, pp. 342–357, 2017, ISSN 1364-0321, <https://doi.org/10.1016/j.rser.2016.11.182>.
- [17] Pennsylvania State University, "The Two Settlement Payment System," <https://www.e-education.psu.edu/ebf483/node/690>.
- [18] Mark Cannon, "Model Predictive Control," Oxford University.
- [19] Awadelrahman, M.A.A., Zong, Y., Li, H.W. and Agert, C., "Economic Model Predictive Control for Hot Water Based Heating Systems in Smart Buildings," *Energy and Power Engineering*, , no. 9, pp. 112–119, 2017, <https://doi.org/10.4236/epe.2017.94B014>.
- [20] Candanedo, Jose and Dehkordi, Vahid R., "Simulation of Model-based Predictive Control Applied to a Solar-assisted Cold Climate Heat Pump System," *International High Performance Buildings Conference*, , no. 149, 2014, <http://docs.lib.purdue.edu/ihpbc/149>.

- [21] Zhun (Jerry) Yu, Gongsheng Huang, Fariborz Haghghat, Hongqiang Li, Guoqiang Zhang, "Control Strategies For Integration of Thermal Energy Storage Into Buildings: State-of-the-Art Review," *Energy and Buildings*, pp. 203–215, 2015, ISSN 0378-7788, <https://doi.org/10.1016/j.enbuild.2015.05.038>.
- [22] M. Miezis, D. Jaunzems, N. Stancioff, "Predictive Control of a Building Heating System," International Scientific Conference - Environmental and Climate Technologies, Riga, Latvia, 10 2016.
- [23] R. P. van Leeuwen, J. Fink and G. J. M. Smit, "Central Model Predictive Control of a Group of Domestic Heat Pumps Case Study for a Small District," 2015 International Conference on Smart Cities and Green ICT Systems (SMARTGREENS), Lisbon, 2015, pp. 1–12.
- [24] D. Fischer, T. Rivera Toral, K.B. Lindberg, B. Wille-Hausmann, H. Madani, "Investigation of Thermal Storage Operation Strategies with Heat Pumps in German Multi Family Houses," *Energy Procedia*, pp. 137–144, 2014, ISSN 1876-6102, <https://doi.org/10.1016/j.egypro.2014.10.420>.
- [25] Thibault Q. Pan, Jaume Salom, Ramon Costa-Castell, "Review of Control Strategies for Improving the Energy Flexibility Provided by Heat Pump Systems in Buildings," *Journal of Process Control*, 2018, ISSN 0959-1524, <https://doi.org/10.1016/j.jprocont.2018.03.006>.
- [26] Andreas Bloess, Wolf-Peter Schill, Alexander Zerrahn, "Power-to-Heat for Renewable Energy Integration: A Review of Technologies, Modeling Approaches, and Flexibility Potentials," *Applied Energy*, vol. 212, pp. 1611–1626, 2018, ISSN 0306-2619, <https://doi.org/10.1016/j.apenergy.2017.12.073>.
- [27] Y. J. Kim, L. K. Norford and J. L. Kirtley, "Modeling and Analysis of a Variable Speed Heat Pump for Frequency Regulation Through Direct Load Control," *IEEE Transactions on Power Systems*, vol. 30, no. 1, pp. 397–408, 1 2015, doi: 10.1109/TSTE.2015.2497407.
- [28] E. Vrettos and G. Andersson, "Scheduling and Provision of Secondary Frequency Reserves by Aggregations of Commercial Buildings," *IEEE Transactions on Sustainable Energy*, vol. 7, no. 2, pp. 850–864, 4 2016, doi: 10.1109/TSTE.2015.2497407.

- [29] X. D. He, *Dynamic Modeling and Multivariable Control of Vapor Compression Cycles in Air Conditioning Systems*, Ph.D. thesis, Massachusetts Institute of Technology, 2 1996, Cambridge, MA, USA.
- [30] B.P. Rasmussen and A.G. Alleyne, *Dynamic Modeling and Advanced Control of Air Conditioning and Refrigeration Systems*, Air Conditioning and Refrigeration Center (ACRC TR-244), 6 2006.
- [31] Wikipedia, "Regions of New York State," [https://en.wikipedia.org/wiki/Category:Regions_of_New_York_\(state\)](https://en.wikipedia.org/wiki/Category:Regions_of_New_York_(state)).
- [32] M. Grant and S. Boyd, "CVX: Matlab Software for Disciplined Convex Programming, Version 2.1, December 2017, Build 1123," <http://cvxr.com/cvx/>.
- [33] Gurobi Optimization, "Mixed-Integer Programming (MIP) - A Primer on the Basics," <http://www.gurobi.com/resources/getting-started/mip-basics>.
- [34] New York State Electric and Gas Corporation, "Electricity Service Rate," Service Class 12, Rate No. 115-12-00.